

Steady State Blended Gas Flow on Networks: Existence and Uniqueness of Solutions

Alena Ulke*, Michael Schuster[†], Simone Göttlich*

November 7, 2024

Abstract. We prove an existence result for the steady state flow of gas mixtures on networks. The basis of the model are the physical principles of the isothermal Euler equation, coupling conditions for the flow and pressure, and the mixing of incoming flow at nodes. The state equation is based on a convex combination of the ideal gas equations of state for natural gas and hydrogen. We analyze mathematical properties of the model allowing us to prove the existence of solutions in particular for tree-shaped networks and networks with exactly one cycle. Numerical examples illustrate the results and explore the applicability of our approach to different network topologies.

AMS Classification. 34B45, 93C15

Keywords. gas pipeline network, gas mixture, hydrogen blending, isothermal Euler equations, stationary states

1 Introduction and Motivation

The transition to renewable energies is one of the most intensively discussed topics in science, with hydrogen being a key element that is set to play an increasingly important role in the global energy mix. Hydrogen offers numerous advantages. Firstly, it is a clean energy source that can be produced using renewable energy sources such as wind and solar power, and its combustion results only in water and heat, [9, 11]. Secondly, hydrogen can be utilized to decarbonize sectors that are difficult to electrify, such as heavy industry [9, 11]. Lastly, hydrogen serves as an energy carrier, making it a valuable resource for energy storage [11, 25]. Given these benefits, there is no doubt that hydrogen will play an important role in the near future.

However, the transition to renewable energies necessitates not only an appreciation of hydrogen's clean energy potential but also a deep understanding of how to integrate it into current energy systems. Even if hydrogen transport networks are planned all over the world

¹University of Mannheim, Department of Mathematics, 68131 Mannheim, Germany (ulke@uni-mannheim.de, goettlich@uni-mannheim.de)

²Friedrich-Alexander University Erlangen-Nürnberg, Department of Mathematics, 91058 Erlangen, Germany (michi.schuster@fau.de)

(cf. [12] for Europe, [23] for Asia, and [31] for U.S.A.), hydrogen is far from completely replacing natural gas as energy source. One key strategy in order to reduce the use of natural gas as energy source as well as to significantly lower the amount of emitted greenhouse gases, is the blending of hydrogen into natural gas networks.

A rigorous mathematical understanding of the hydrogen-natural gas blending processes is essential for the efficiency and safety of existing pipeline networks. Compared to the transport of pure hydrogen, the complexity lies in modelling and understanding the mixing of two gases. While the transport of pure hydrogen as well as pure natural gas in pipeline networks can be modeled by the isothermal Euler equations, cf. [3, 10, 22], a different approach is needed for the modelling of gas mixtures. Since natural gas has been and still is widely used as an energy source for decades almost all over the world, researchers can rely on well-established regulations for natural gas networks and extensive research in this area. In [26], the authors discuss stationary states of the isothermal Euler equations and in [16] the existence of unique stationary states was shown on arbitrary graphs. In [2, 3] the authors analyze the transient model and discuss solutions to Riemann problems on arbitrary graphs including appropriate coupling conditions at the nodes, i.e., conservation of mass and pressure continuity. Further, the existence of semi-global Lipschitz continuous solutions of the isothermal Euler Equations on a network with compatible coupling conditions was shown in [18], based on a fixed point iteration along the characteristic curves for Lipschitz continuous initial and boundary conditions.

However, applying the isothermal Euler equations for both, hydrogen and natural gas in the same pipeline, does not consider collisions of molecules of different types, which leads to adulterated results [20]. Based on the analysis of chemical reacting fluid mixtures in [8, 24] we consider a model for the flow of a natural gas and hydrogen mixture under perfect mixing conditions (i.e., both gases have the same velocity and temperature), given by

$$\frac{\partial}{\partial t}\rho_{\text{NG}}(t, x) + \frac{\partial}{\partial x}q_{\text{NG}}(t, x) = 0, \quad (1.1a)$$

$$\frac{\partial}{\partial t}\rho_{\text{H}_2}(t, x) + \frac{\partial}{\partial x}q_{\text{H}_2}(t, x) = 0, \quad (1.1b)$$

$$\frac{\partial}{\partial t}q(t, x) + \frac{\partial}{\partial x}\left[p(\rho_{\text{NG}}(t, x), \rho_{\text{H}_2}(t, x)) + \frac{q^2(t, x)}{\rho(t, x)}\right] = -\frac{\lambda_{\text{Fr}}}{2D}\frac{q(t, x)|q(t, x)|}{\rho(t, x)}, \quad (1.1c)$$

where $\rho_{\text{NG}}, \rho_{\text{H}_2}$ are the densities of natural gas and hydrogen, $q_{\text{NG}}, q_{\text{H}_2}$ are the flows of natural gas and hydrogen, p, ρ, q are the pressure, flow and density of the mixture, $\lambda_{\text{Fr}} > 0$ is the pipe friction coefficient and D is the pipe diameter. The pressure of the mixture depends on the densities by the state equation derived for example in [7] for the mixture of ideal gases and in [6] for the mixture of real gases. The latter also assumes a non-isothermal dynamic.

The mixing model (1.1) on networks also includes coupling conditions at the network junctions. For natural gas transport on networks, conservation of mass and continuity of the pressure are typical choices, cf. [16, 17, 27, 30]. In [2], the authors give an overview of coupling conditions for models of natural gas transport on networks. In the mixing model (1.1), we also consider perfect mixing at the nodes, which implies that the outgoing hydrogen concentration is equal to the average weighted by the flow of all ingoing concentrations.

For the long time horizon planning of gas networks, dynamic models are often replaced by static models, that represent the steady states, cf. [16, 17, 20, 26, 30]. Simulation results for models based on (1.1) and corresponding steady state models were presented, for example, in

[14, 20, 33]. Considering natural gas and hydrogen as ideal gases, in [15] the authors present a well-posedness result of (1.1) under the assumption, that the hydrogen concentration is sufficiently low. To our best knowledge, neither the existence of steady states for the mixing model (1.1), nor steady states for the mixing on networks were theoretically analyzed yet. The only result that fits into this line of research is that for tree-shaped networks steady state solutions are unique if they exist, cf. [20]. However, proving uniqueness becomes more intricate for networks with cycles, since the monotonicity of the pressure, which guarantees the uniqueness for pure natural gas transport, is unclear a priori due to the mixing.

In this paper, we present an analytic solution of the steady states of (1.1). Further, we analyze the existence and uniqueness of steady states for the hydrogen blended natural gas flow on networks. We discuss tree-shaped pipeline networks as well as networks that contain cycles. For pure gas flow the existence and uniqueness of steady states was analyzed in [16] for ideal gases and in [32] for real gases. In the case of gas mixtures, the gas composition in a pipeline depends on the direction of the flow, which leads to discontinuities in the mixing model if the graph contains cycles. We present a novel existence result for steady states of the mixing model for networks with a cycle. The result is based on cutting edges of the cycle such that the model has a solution on the resulting tree-shaped network with new supply and demand nodes. The challenge here lies in the discontinuity of the composition of the new supply and demand nodes, which underlines the difficulty compared to pure natural gas networks, where this discontinuity does not occur.

The article structures as follows: First, we introduce and motivate the gas flow model for mixtures on networks in Section 2. We also show that certain properties of the gas flow of a single gas carries over to the gas flow of mixtures. Then, in Section 3, we establish the existence of steady state solutions for tree-shaped networks and networks with a single cycle. Finally, we conclude with a numerical study in Section 4, which analyzes whether the idea of the existence result also extends to networks with arbitrarily many cycles and whether the solutions are unique.

2 The Model Equations on Networks

In this section, we derive a steady-state model for the hydrogen blended natural gas flow in pipeline networks. We further define suitable boundary and coupling conditions for the flow, the pressure and the composition of the gas mixture at the junctions of the network.

Throughout this paper we assume that $\mathcal{G} = (\mathcal{V}, \mathcal{E})$ is a connected, directed graph with nodes $v \in \mathcal{V}$ and edges $e \in \mathcal{E} \subseteq \mathcal{V} \times \mathcal{V}$. Each edge e represents a pipe of length L^e and each node v represents a junction where pipes meet. We consider two types of nodes:

- (i) *inflow* or *supply nodes* $v \in \mathcal{V}_{<0}$, where gas enters the network,
- (ii) *outflow* or *demand nodes* $v \in \mathcal{V}_{\geq 0}$, where gas leaves the network or the mass is conserved,

This classification of nodes satisfies $\mathcal{V} = \mathcal{V}_{<0} \cup \mathcal{V}_{\geq 0}$ with $\mathcal{V}_{<0} \cap \mathcal{V}_{\geq 0} = \emptyset$. For every node $v \in \mathcal{V}$, the set of *incoming* and *outgoing edges* are given by

$$\mathcal{E}_-(v) := \{e \in \mathcal{E} \mid e = (\bullet, v)\} \quad \text{and} \quad \mathcal{E}_+(v) := \{e \in \mathcal{E} \mid e = (v, \bullet)\},$$

respectively. The set containing all edges incident to v is given by $\mathcal{E}(v) = \mathcal{E}_-(v) \cup \mathcal{E}_+(v)$. For edges $e \in \mathcal{E}_-(v)$, the node v is their *head* or *end node* and for edges $e \in \mathcal{E}_+(v)$, the node v is

their *foot* or *start node*. In the following, we denote the head of an edge by $h(e)$ and the foot of an edge by $f(e)$, i.e., we have

$$e = (v, w) \Leftrightarrow f(e) = v \quad \text{and} \quad h(e) = w.$$

Further let $A \in \mathbb{R}^{|\mathcal{V}| \times |\mathcal{E}|}$ be the so-called *node edge incidence matrix*, whose entries are defined by

$$a(v, e) := \begin{cases} -1, & \text{if } v = f(e), \text{ i.e., } v \text{ is the start node of } e, \\ 1, & \text{if } v = h(e), \text{ i.e., } v \text{ is the end node of } e, \\ 0, & \text{otherwise.} \end{cases} \quad (2.1)$$

2.1 The Isothermal Euler Equations for Mixtures

To model the flow of a mixture through a pipe e , we consider the steady-state hydrogen blended gas flow model corresponding to the transient model (1.1). Additionally, we neglect the term q_e^2/ρ_e in the differential equation for the pressure p_e compared to the transient model (1.1) as the velocity of the gas flow is significantly smaller than the speed of sound. Thus, we are in a subsonic regime since the Mach number is sufficiently small. Then, the subsonic steady-state hydrogen blended gas flow model reads:

$$\partial_x q_{\text{NG}}^e(x) = 0, \quad \text{for } x \in [0, L^e] \quad (2.2a)$$

$$\partial_x q_{\text{H}_2}^e(x) = 0, \quad \text{for } x \in [0, L^e] \quad (2.2b)$$

$$\partial_x p_e(\rho_{\text{NG}}^e(x), \rho_{\text{H}_2}^e(x)) = -\frac{\lambda_{\text{Fr}} q_e(x) |q_e(x)|}{2D \rho_e(x)}, \quad \text{for } x \in [0, L^e] \quad (2.2c)$$

where ρ_{NG}^e and $\rho_{\text{H}_2}^e$ denote the density and q_{NG}^e and $q_{\text{H}_2}^e$ the flow of natural gas and hydrogen along the pipe. The constant $\lambda_{\text{Fr}} > 0$ denotes the friction factor and D the diameter of the pipe. For the reader's convenience we assume the same friction and diameter for every pipe. Moreover, ρ_e describes the density, q_e the flow, η_e describes the composition, and p_e the pressure of the mixture along the pipe $e \in \mathcal{E}$. These quantities are defined as

$$\rho_e(x) = \rho_{\text{H}_2}^e(x) + \rho_{\text{NG}}^e(x), \quad q_e(x) = q_{\text{H}_2}^e(x) + q_{\text{NG}}^e(x), \quad \eta_e(x) = \frac{q_{\text{H}_2}^e(x)}{q_e(x)} = \frac{\rho_{\text{H}_2}^e(x)}{\rho_e(x)},$$

while the latter holds due to the assumption that both gases have the same velocity. For the pressure law we assume that the gases and their mixture are ideal which leads to

$$p_e(\rho_{\text{NG}}^e(x), \rho_{\text{H}_2}^e(x)) = \left[\eta_e(x) \sigma_{\text{H}_2}^2 + (1 - \eta_e(x)) \sigma_{\text{NG}}^2 \right] \rho_e(x), \quad (2.3)$$

where $\sigma_{\text{H}_2}^2 = R_{S, \text{H}_2} T$ is the speed of sound in hydrogen and $\sigma_{\text{NG}}^2 = R_{S, \text{NG}} T$ is the speed of sound in natural gas. Moreover, R_{S, H_2} and $R_{S, \text{NG}}$ are the specific gas constants of hydrogen and natural gas, respectively, and T the temperature of the gas. Then, the solution to the system of ordinary differential equations (2.2) describing the gas flow of a hydrogen-natural

gas mixture along a pipe, reads:

$$q_{\text{NG}}^e(x) = \text{const}, \quad q_{\text{H}_2}^e(x) = \text{const}, \quad (2.4a)$$

$$p_e(x) = \sqrt{\left[p_e^2(0) - \frac{\lambda_{\text{Fr}}}{D} (\eta_e \sigma_{\text{H}_2}^2 + (1 - \eta_e) \sigma_{\text{NG}}^2) q_e |q_e| x \right]}. \quad (2.4b)$$

The flow of hydrogen and natural gas is constant along the pipe and the pressure is uniquely defined by the pressure at the beginning and the end of the pipe. If $p_e(0)$ is given for an edge $e \in \mathcal{E}$, the the critical length of the pipe is given by

$$L_{\text{crit}}^e = \frac{p_e^2(0)}{\frac{\lambda_{\text{Fr}}}{D} (\eta_e \sigma_{\text{H}_2}^2 + (1 - \eta_e) \sigma_{\text{NG}}^2) q_e |q_e|}, \quad (2.5)$$

which means that if $L^e > L_{\text{crit}}^e$, then a solution of p_e does not exist in \mathbb{R} . For the sake of better readability, we omit the dependence of the spatial variable x in the following.

2.2 Boundary and Coupling Conditions for the Nodes

As gas is injected or withdrawn from the network at the nodes, we introduce the load vector $\mathbf{b} \in \mathbb{R}^{|\mathcal{V}|}$ with entries

$$b_v \begin{cases} < 0 & \text{if } v \in \mathcal{V}_{<0}, \text{ which means } v \text{ is a supply node,} \\ \geq 0 & \text{if } v \in \mathcal{V}_{\geq 0}, \text{ which means } v \text{ is a demand node,} \end{cases} \quad (2.6)$$

describing the supply and demand of a node v . The case $b_v = 0$ implies, that gas is neither injected nor withdrawn from node v .

For the boundary conditions, we provide the load b_v at each node $v \in \mathcal{V}$. At supply nodes $v \in \mathcal{V}_{<0}$, we additionally specify the supply composition ζ_v . Furthermore, we provide the pressure p^* at an arbitrary yet fixed node $v^* \in \mathcal{V}$, i.e., we set $p_{v^*} = p^*$.

For the coupling conditions, we make three assumptions to describe the gas flow across nodes:

- (i) The mass of the mixture and the mass of the individual gases are conserved,
- (ii) the gas mixes instantaneously and perfectly, and
- (iii) the pressure is continuous across a node.

The first assumption, the conservation of mass at a node $v \in \mathcal{V}$ means, that the amount of gas entering node v must be equal to the amount of gas leaving node v including the supply and demand of the node, respectively, i.e., we have

$$\sum_{e \in \mathcal{E}_+(v)} q_e - \sum_{e \in \mathcal{E}_-(v)} q_e = b_v.$$

Using the incidence matrix A defined in Equation (2.1), the conservation of mass of the mixture at all nodes $v \in \mathcal{V}$, is given by

$$\sum_{e \in \mathcal{E}(v)} a(v, e) q_e = b_v \quad \text{for all } v \in \mathcal{V} \quad \Leftrightarrow \quad A \mathbf{q} = \mathbf{b}, \quad (2.7)$$

where $\mathbf{q} \in \mathbb{R}^{|\mathcal{E}|}$ is the vector of (constant) flows at the edges.

Remark 2.1. Due to the conservation of mass and the definition of the incidence matrix A , the loads b_v must sum up to zero, i.e., we have

$$\sum_{v \in \mathcal{V}} b_v = 0. \quad (2.8)$$

Hence, it is sufficient to provide the loads b_v for $|\mathcal{V}| - 1$ nodes as the missing load is automatically determined by Equation (2.8).

Next, we discuss the perfect mixing at the nodes, which implies that the incoming gas compositions at a node v are weighted by the respective incoming flows and are then averaged and that the composition of all outgoing flows is equal. Hence, we introduce the nodal composition η_v of the gas at a node $v \in \mathcal{V}$:

$$\eta_v = \frac{\text{incoming hydrogen}}{\text{outgoing gas}} = \frac{\text{incoming hydrogen}}{\text{incoming gas}},$$

while the latter holds due to the conservation of mass. In Figure 1, we provide an example on how to compute the nodal composition at a node v depending on whether the node is a supply or a demand node.

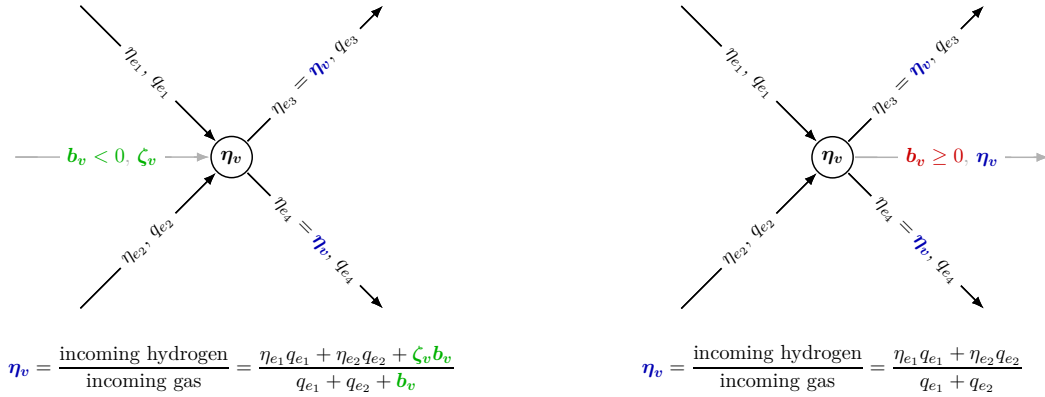


Figure 1: The mixing of gas for a supply node (left) and a demand node (right). The supply and demand of a node can be seen as an invisible pipe with fixed flow.

Remark 2.2. At a supply node $v \in \mathcal{V}_{<0}$, the nodal composition η_v differs from the composition ζ_v of the supply because the supply at the node mixes with the inflow from incident pipes first, resulting in the nodal composition η_v . As the individual compositions of the inflow differs for every pipe in general, their weighted average, the composition η_v , differs from the supply composition ζ_v , cf. Figure 1. The relation $\eta_v = \zeta_v$ only holds for supply nodes $v \in \mathcal{V}_{<0}$ satisfying $|\mathcal{E}(v)| = 1$.

As the flow direction might differ from the orientation of the edge, it is unclear a priori which pipes carry incoming and which pipes carry outgoing gas. However, we can use the incidence matrix to determine whether a given flow q_e of an edge $e \in \mathcal{E}(v)$ is directed in or

away from the node v :

$$\begin{aligned} a(v, e) q_e \leq 0 &\Leftrightarrow \text{Gas in pipe } e \text{ flows towards node } v. \\ a(v, e) q_e \geq 0 &\Leftrightarrow \text{Gas in pipe } e \text{ flows away from } v. \end{aligned} \quad (2.9)$$

We provide a visualization of the condition (2.9) in Figure 2. For a number α , we define $\alpha^+ = \max\{\alpha, 0\}$ and $\alpha^- = \max\{-\alpha, 0\}$. Then, the nodal composition at a node $v \in \mathcal{V}$ is given by

$$\eta_v = \frac{\sum_{e \in \mathcal{E}(v)} \eta_e \cdot (a(v, e) q_e)^+ + \zeta_v b_v^-}{\sum_{e \in \mathcal{E}(v)} (a(v, e) q_e)^+ + b_v^-}, \quad (2.10)$$

where η_e is the composition along the pipe e . There is an explicit relation between the nodal composition η_v and the composition along a pipe η_e since the nodal composition η_v is transferred to all pipes $e \in \mathcal{E}(v)$ carrying outgoing flow. More specifically, we have

$$\eta_e = \begin{cases} \eta_{f(e)} & \text{if } q_e \geq 0, \\ \eta_{h(e)} & \text{if } q_e < 0, \end{cases} \quad \text{for all } e \in \mathcal{E}, \quad (2.11)$$

which means that the composition along the edge e is given by the nodal composition at the start node $f(e)$ of the edge if the flow q_e is directed away from $f(e)$, and by nodal composition at the end node $h(e)$ if the flow q_e is directed away from $h(e)$. The relation (2.11) allows us to express the computation of the nodal composition η_v fully in terms of nodal compositions, cf. Equation (2.10):

$$\eta_v = \frac{\sum_{e \in \mathcal{E}(v)} \eta_{w_e} (a(v, e) q_e)^+ + \zeta_v b_v^-}{\sum_{e \in \mathcal{E}(v)} (a(v, e) q_e)^+ + b_v^-} \quad \text{where } w_e = \begin{cases} f(e), & \text{if } v = h(e), \\ h(e), & \text{if } v = f(e). \end{cases}$$

The node w_e of an edge $e \in \mathcal{E}(v)$ incident to v , is the node that is not v , i.e., if v is the start node of e then w_e is the end node of e and if v is the end node then w_e is the start node.



- (a) The flow q_e is directed into a node v , i.e., an inflow, if and only if $a(v, e) q_e \geq 0$. (b) The flow q_e is directed away from a node v , i.e., an outflow, if and only if $a(v, e) q_e \leq 0$.

Figure 2: The four possible relations between flow and edge direction, cf. Equation (2.9).

At last, we discuss the continuity of the pressure across a node. This means, that for all

nodes $v \in \mathcal{V}$ and all incident edges $e, \tilde{e} \in \mathcal{E}(v)$ the following condition holds:

$$p_e(x_e) = p_{\tilde{e}}(x_{\tilde{e}}) \quad \text{where} \quad x_e = \begin{cases} 0, & e \in \mathcal{E}_-(v), \\ L^e, & e \in \mathcal{E}_+(v). \end{cases}$$

As the pressure loss along a pipe is defined by Equation (2.4), we ensure the continuity of the pressure across a node by introducing the nodal pressure p_v for each node v . Then, Equation (2.4) is given by

$$p_{h(e)}^2 - p_{f(e)}^2 = -\frac{\lambda_{\text{Fr}}}{D} \left(\eta_e \sigma_{\text{H}_2}^2 + (1 - \eta_e) \sigma_{\text{NG}}^2 \right) q_e |q_e| L^e \quad \text{for all } e \in \mathcal{E}.$$

As the composition η_e on an edge is discontinuous in $q_e = 0$, cf. Equation (2.11), the pressure p_e is discontinuous in $q_e = 0$ as well. However, for pure natural gas transport, the pressure continuously depends on the nodal pressure and on the gas flow, see for example [19, 32]. As the continuity will be crucial for our further analysis, we rewrite by expressing the pressure loss in terms of the nodal composition instead of the composition on the edges. First, we rewrite

$$\begin{aligned} \eta_e \sigma_{\text{H}_2}^2 + (1 - \eta_e) \sigma_{\text{NG}}^2 &= \frac{1}{2} \left(\frac{|q_e|}{q_e} + 1 \right) \sigma(\eta_{f(e)}) - \frac{1}{2} \left(\frac{|q_e|}{q_e} - 1 \right) \sigma(\eta_{h(e)}) \quad \text{for } e \in \mathcal{E}, \\ \text{where } \sigma(\eta_v) &:= \eta_v \sigma_{\text{H}_2}^2 + (1 - \eta_v) \sigma_{\text{NG}}^2 \quad \text{for } v \in \mathcal{V}. \end{aligned}$$

Then, for each edge $e \in \mathcal{E}$ we define

$$\tilde{\sigma}(\eta_{f(e)}, \eta_{h(e)}, q_e) := -\frac{\lambda_{\text{Fr}}}{D} L^e \left[\frac{1}{2} \left(\frac{|q_e|}{q_e} + 1 \right) \sigma(\eta_{f(e)}) - \frac{1}{2} \left(\frac{|q_e|}{q_e} - 1 \right) \sigma(\eta_{h(e)}) \right], \quad (2.12)$$

which allows to derive an expression of the pressure loss along a pipe in terms of the nodal compositions with removable singularity:

$$p_{h(e)}^2 - p_{f(e)}^2 = \tilde{\sigma}(\eta_{f(e)}, \eta_{h(e)}, q_e) q_e |q_e| \quad \text{for all } e \in \mathcal{E}. \quad (2.13)$$

In the following, we will use Equation (2.13) to describe the pressure loss along a pipe.

2.3 The Full Model on Graphs

The full steady state gas flow model for gas mixtures consists of the pressure loss along a pipe, the conservation of mass across nodes, the mixing of the gases at nodes, and the boundary conditions defined above.

For each node $v \in \mathcal{V}$, we specify its load b_v , which must satisfy $\sum_{v \in \mathcal{V}} b_v = 0$. Further, we provide the supply composition ζ_v at supply nodes $v \in \mathcal{V}_{<0}$, and fix a single nodal pressure $p_{v^*} = p^*$ at an arbitrary node $v^* \in \mathcal{V}$. For these given values, the gas flow model for mixtures

is given by

$$p_{h(e)}^2 - p_{f(e)}^2 = \tilde{\sigma}(\eta_{f(e)}, \eta_{h(e)}, q_e) q_e |q_e| \quad \text{for all } e = (f(e), h(e)) \in \mathcal{E}, \quad (2.14a)$$

$$A\mathbf{q} = \mathbf{b} \quad \text{for all } v \in \mathcal{V}, \quad (2.14b)$$

$$\eta_v = \frac{\sum_{e \in \mathcal{E}(v)} \eta_e \cdot (a(v, e) q_e)^+ + \zeta_v b_v^-}{\sum_{e \in \mathcal{E}(v)} (a(v, e) q_e)^+ + b_v^-} \quad \text{for all } v \in \mathcal{V}. \quad (2.14c)$$

The first equation (2.14a) describes the pressure loss along the pipes and guarantees the pressure continuity across nodes. The second equation (2.14b) ensures the mass conservation at the nodes and describes the injection and withdrawal of gas from the network at the nodes. The last equation (2.14c) describes the perfect mixing at the nodes and guarantees the conservation of mass for the individual gases, i.e., natural gas and hydrogen, across nodes.

Remark 2.3. A small computation shows that the mixture model (2.14) corresponds to the one presented in [7] even though the derivations are different at a first glance.

2.4 Properties of the Gas Flow

For gas flow with only a single gas, the gas cannot flow in cycles in networks without compressor stations, cf. [16]. This property carries over to the gas flow of mixtures and we will need this property later when proving that the mixture model (2.14) admits at least one solution. To prove that the mixture model (2.14) does not allow circular flows, we determine the pressure loss along a path connecting two nodes first as a cycle is a path with identical start and end node.

Lemma 2.4 (Pressure Loss Along a Path). *Let $\mathcal{G} = (\mathcal{V}, \mathcal{E})$ be a connected graph and let $(\mathcal{P}, \mathcal{E}_{\mathcal{P}})$ be a path starting at node v_0 and ending at node v_k where $\mathcal{P} = \{v_0, \dots, v_k\}$ and $\mathcal{E}_{\mathcal{P}}$ contains the edges connecting two consecutive nodes v_i and v_{i+1} . Then the pressure loss along the path is given by*

$$p_{v_k}^2 - p_{v_0}^2 = \sum_{e \in \mathcal{E}_{\mathcal{P}}} \tilde{\sigma}(\eta_{h(e)}, \eta_{f(e)}, q_e) a(v_e, e) q_e |a(v_e, e) q_e|,$$

where the node v_e is the node of edge e that is closer to the start node v_0 of the path, i.e., $v_e = f(e)$ if $e = (v_i, v_{i+1})$ and $v_e = h(e)$ if $e = (v_{i+1}, v_i)$.

Proof. We prove the claim by rewriting the pressure loss between two consecutive nodes v_k and v_{k+1} of the path, i.e., the pressure loss along the pipe connecting v_k and v_{k+1} :

$$\begin{aligned} p_{v_{k+1}}^2 &= \begin{cases} p_{v_k}^2 - \tilde{\sigma}(\eta_{v_k}, \eta_{v_{k+1}}, q_e) q_e |q_e|, & \text{if } e = (v_k, v_{k+1}) \\ p_{v_k}^2 + \tilde{\sigma}(\eta_{v_{k+1}}, \eta_{v_k}, q_e) q_e |q_e|, & \text{if } e = (v_{k+1}, v_k) \end{cases} \\ &= \begin{cases} p_{v_k}^2 + \tilde{\sigma}(\eta_{f(e)}, \eta_{h(e)}, q_e) a(v_k, e) q_e |a(v_k, e) q_e|, & \text{if } e = (v_k, v_{k+1}) \\ p_{v_k}^2 + \tilde{\sigma}(\eta_{f(e)}, \eta_{h(e)}, q_e) a(v_{k+1}, e) q_e |a(v_{k+1}, e) q_e|, & \text{if } e = (v_{k+1}, v_k) \end{cases} \\ &= p_{v_k}^2 + \tilde{\sigma}(\eta_{f(e)}, \eta_{h(e)}, q_e) a(v_e, e) q_e |a(v_e, e) q_e|, \end{aligned}$$

Then, the claim follows by an induction over the path length $|\mathcal{E}_{\mathcal{P}}|$. \square

A cycle is a path with identical start and end node. Since gas flowing in cycles means that the gas always flows either away from or into the node when traversing through the cycle starting from a designated start node, we use Equation (2.9) to characterize circular flows, cf. Figure 3 for a visualization. The designated „start node“ can be any node in the cycle.

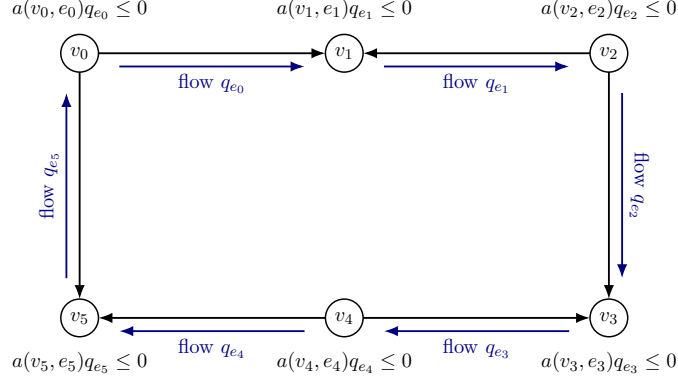


Figure 3: Illustration of a circular flow moving clockwise „starting“ from node v_0 . The edge direction is marked in black and the flow direction in blue.

Corollary 2.5. *Let $\mathcal{G} = (\mathcal{V}, \mathcal{E})$ be a connected graph. Then a solution to the gas flow model (2.14) does not allow circular flows, i.e., there exists no circle $(\mathcal{C}, \mathcal{E}_{\mathcal{C}})$ in the network satisfying one of the following two conditions:*

- (i) $a(v_e, e) q_e \geq 0$ for all $e \in \mathcal{E}_{\mathcal{C}}$ and $a(v_e, e) q_e > 0$ for at least one $e \in \mathcal{E}_{\mathcal{C}}$,
- (ii) $a(v_e, e) q_e \leq 0$ for all $e \in \mathcal{E}_{\mathcal{C}}$ and $a(v_e, e) q_e < 0$ for at least one $e \in \mathcal{E}_{\mathcal{C}}$,

where $v_e \in \mathcal{V}$ is incident to e and the node closest to the start node while ignoring the edge between start and end node, cf. Lemma 2.4.

Proof. We assume the contrary and prove for the first case (i). A circle $(\mathcal{C}, \mathcal{E}_{\mathcal{C}})$ is a path with identical start and end node. Thus, applying Lemma 2.4 yields:

$$0 = p_{v_k}^2 - p_{v_0}^2 = \sum_{e \in \mathcal{E}_{\mathcal{C}}} \underbrace{\tilde{\sigma}(\eta_{f(e)}, \eta_{h(e)}, q_e)}_{\geq 0} \underbrace{a(v_e, e) q_e}_{\geq 0} \underbrace{|a(v_e, e) q_e|}_{\geq 0} \stackrel{(*)}{>} 0,$$

which is a contradiction. The strict inequality $(*)$ holds because there exists at least one edge $e \in \mathcal{E}_{\mathcal{C}}$ satisfying $a(v_e, e) q_e > 0$. The proof for the second case (ii) follows analogously. \square

3 The Existence and Uniqueness of Steady States on Networks

In this section, we prove the existence of steady states on networks for the mixture model (2.14). The idea follows [19, 32] where the authors prove the existence of steady states on networks for the „classic“ gas flow model involving only a single gas. Their proof is based on an induction over the number of cycles in a graph. To apply the induction assumption, one cuts an edge of a cycle to obtain a graph, that has one cycle less than the original one.

Thus, we first show the existence and uniqueness of solutions of the mixture model (2.14) on tree-shaped networks, i.e., network with no cycles, and establish the existence of steady-states for networks with cycles afterwards.

3.1 Steady States on Tree-Shaped Networks

The existence and uniqueness of steady states for tree-shaped networks is, similar to the single gas problem, straightforward as the argument only relies on the fact that for trees, the flow on the network is fully determined by the loads b_v . However, we have one additional equation to describe the mixing at nodes. Provided that the mixing equation (2.14c) admits a unique solution, the proof to show the existence and uniqueness of steady states on tree-shaped networks is analogous to the proof of the steady-state gas flow model with a single gas.

We can compute the composition η_v at a node v if we know its incoming flows and their composition since the nodal composition η_v is given by the ratio of the incoming hydrogen and incoming gas, cf. Equation (2.14c). As the network is tree-shaped, we can sort the nodes such that gas always flows from nodes early in the ordering to nodes later in the ordering what allows us to compute the nodal compositions η_v in an inductive manner. Such an ordering of the nodes is called a *topological ordering* of a graph.

Definition 3.1 (Topological Ordering [4]). Let $\mathcal{G} = (\mathcal{V}, \mathcal{E})$ be a directed, tree-shaped graph. Then a *topological ordering* of a directed graph sorts the nodes of the graph into a sequence in which, for each directed edge (v, w) , the start node v appears before the end node w , cf. Figure 4 for a visualization.

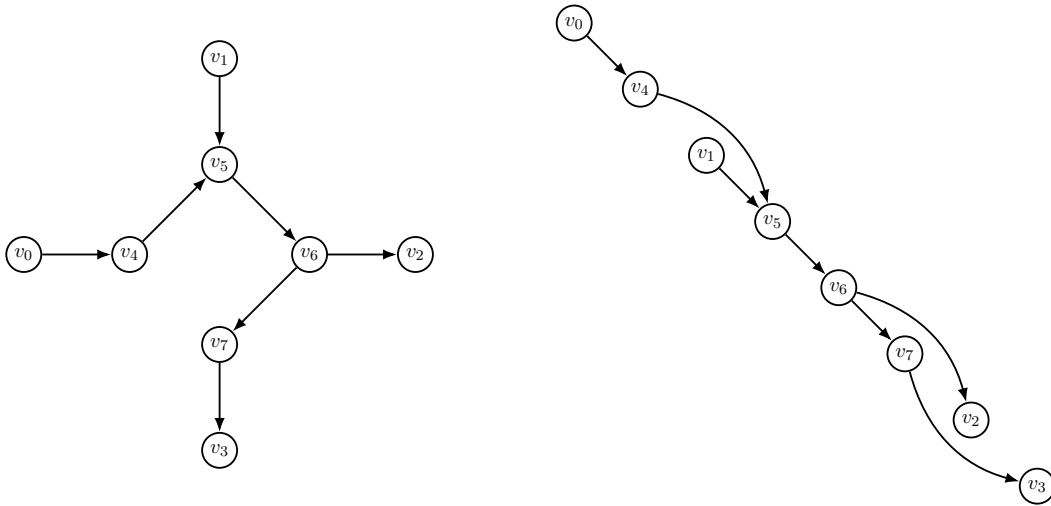


Figure 4: A directed acyclic graph (left) and a topological ordering of its nodes (right).

To compute the compositions η_v for fixed flows q_e , we require a topological ordering of the graph $\mathcal{G}_{\text{flow}} = (\mathcal{V}, \mathcal{E}_{\text{flow}})$, which has the same nodes as \mathcal{G} but edges according to the flow direction, i.e., its edges are defined by

$$(v, w) \in \mathcal{E}_{\text{flow}} \quad :\Leftrightarrow \quad \begin{cases} (v, w) \in \mathcal{E}, & \text{if } q_e \geq 0, \\ (w, v) \in \mathcal{E}, & \text{if } q_e < 0. \end{cases} \quad (3.1)$$

A topological ordering of the graph \mathcal{G} implies that pipes start at nodes early in the ordering and end at nodes later in the ordering, as the flow direction may differ from the pipe orientation. This can lead to gas flowing from nodes later in the ordering to nodes earlier in the ordering, which is undesired. However, a topological ordering of $\mathcal{G}_{\text{flow}}$ guarantees that gas always flows from nodes early in the ordering to nodes later in the ordering, which is what we require.

Note that the graph $\mathcal{G}_{\text{flow}}$ emerges from the original graph \mathcal{G} by flipping edges where the flow and edge direction differ. Hence, the graph $\mathcal{G}_{\text{flow}}$ depends on the flow q_e on the edges. We provide an example of the relation between the graph \mathcal{G} and the graph $\mathcal{G}_{\text{flow}}$ in Figure 5.

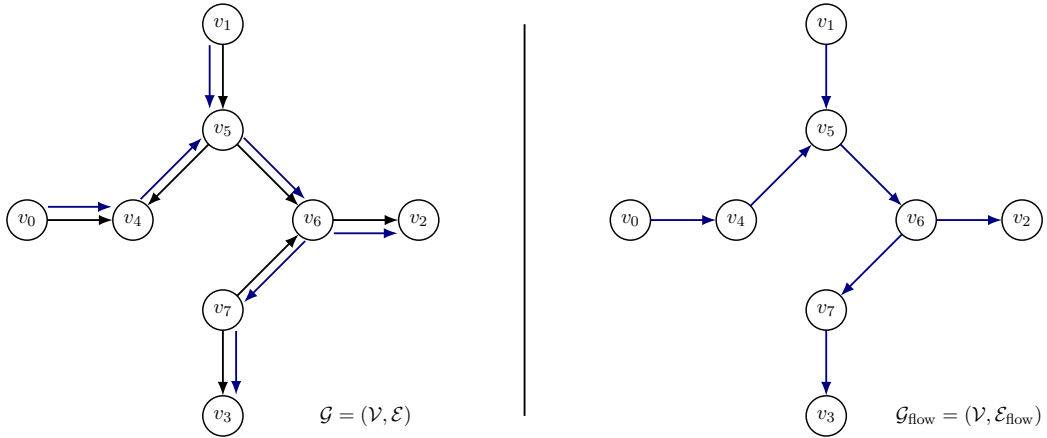


Figure 5: A directed graph \mathcal{G} in black, given flow q_e on the edges in blue (left) and the graph $\mathcal{G}_{\text{flow}}$ with edges according to the flow direction (right).

Remark 3.2. The graph $\mathcal{G}_{\text{flow}}$ is tree-shaped because it has the same edge as \mathcal{G} up to a change in the edge orientation and thus, by [4, Proposition 2.1.3] there exists a topological ordering of the nodes of $\mathcal{G}_{\text{flow}}$.

Therefore, we are now equipped to show the existence of a solution to the mixing equation (2.14c) given fixed flows q_e on a network.

Lemma 3.3 (Existence of the Composition). *Let $\mathcal{G} = (\mathcal{V}, \mathcal{E})$ be a directed graph and let q_e be flows on the graph satisfying mass conservation, cf. Equation (2.14b). Then the mixing equation (2.14c) has at least one solution η_v .*

Proof. The graph $\mathcal{G}_{\text{flow}} = (\mathcal{V}, \mathcal{E}_{\text{flow}})$ (cf. Equation (3.1) for the definition) is acyclic. Thus, there exists a topological ordering of the nodes of $\mathcal{G}_{\text{flow}}$ and we can compute the nodal compositions η_v by induction over the position k in the topological ordering.

The composition η_v for the node at position $k = 1$ is given by boundary data since the first node in a topological ordering has to be a supply node, i.e., $b_v < 0$, where $a(v, e)q_e \leq 0$ for all $e \in \mathcal{E}(v)$, and thus $\eta_v = \zeta_v$.

Now assume all nodal compositions up to position k have been determined. Then we compute the composition of the node at position $k + 1$ by invoking

$$\eta_v = \frac{\sum_{e \in \mathcal{E}(v)} \eta_e \cdot (a(v, e)q_e)^+ + \zeta_v b_v^-}{\sum_{e \in \mathcal{E}(v)} (a(v, e)q_e)^+ + b_v^-}.$$

The incoming flow, i.e., edges with $(a(v, e)q_e)^+ \neq 0$, only comes from nodes previous in the ordering. Assume otherwise then there exists an edge whose end point comes before the start point in the ordering which is a contradiction to the definition of a topological ordering. \square

The proof of the existence of a solution relies on a topological ordering of the nodes. Since this ordering is in general non-unique, the question arises whether the solution depends on the topological ordering used to traverse through the nodes. Fortunately, this is not the case, since the solution to the mixing equation is unique.

Lemma 3.4 (Uniqueness of the Composition). *Let $\mathcal{G} = (\mathcal{V}, \mathcal{E})$ be a directed, tree-shaped graph and let q_e be an flows on the graph satisfying the mass conservation, cf. Equation (2.14b). Then the solution η_v to the mixing equation (2.14c) is unique.*

Proof. Follows directly from [20, Theorem 1]. \square

Finally, we prove the existence and uniqueness of solution to the steady-state gas flow model (2.14) for tree-shaped networks.

Theorem 3.5 (Existence of Solutions for Tree-Shaped Networks). *Let $\mathcal{G} = (\mathcal{V}, \mathcal{E})$ be a tree-shaped network. Then the mixture model (2.14) admits a unique solution.*

Proof. As the network \mathcal{G} is tree-shaped, the incidence matrix A has full column rank [5, Lemma 2.2] and thus, the flow equation $A\mathbf{q} = \mathbf{b}$ has a unique solution if and only if

$$\sum_{v \in \mathcal{V}} b_v = 0.$$

Since the loads b_v satisfies this condition by assumption, the flow equation has a unique solution \mathbf{q} that depends only on the nodal flow rates and the topology of the network. Hence, by Lemma 3.3 and Lemma 3.4, the mixing equation (2.14c) has a unique solution given the solution \mathbf{q} of the flow equation.

Together with the fixed nodal pressure p_v at the node v^* , we rewrite Equation (2.14a), which describes the pressure loss along the pipes using the incidence matrix. This yields the following linear system:

$$A^\top \mathbf{p}^2 = \tilde{\boldsymbol{\sigma}}(\boldsymbol{\eta}, \mathbf{q}) \quad \text{with} \quad p_{v^*} = p^* \quad (3.2a)$$

$$\Leftrightarrow A_{-v^*}^\top \mathbf{p}_{-v^*}^2 = \underbrace{\tilde{\boldsymbol{\sigma}}(\boldsymbol{\eta}, \mathbf{q}) - (p^*)^2 \mathbf{a}_{v^*}}_{\text{fully determined}}, \quad (3.2b)$$

where A_{-v^*} and \mathbf{p}_{-v^*} are the incidence matrix A and the vector \mathbf{p} , but without the row and entry corresponding v^* , respectively, and \mathbf{a}_{v^*} denotes the row of A corresponding to v^* . Moreover, the function $\tilde{\boldsymbol{\sigma}}$ is the vector-valued version of the function $\tilde{\sigma}$ defined in Equation (2.12), which means the vector $\tilde{\boldsymbol{\sigma}}(\boldsymbol{\eta}, \mathbf{q}) \in \mathbb{R}^{|\mathcal{E}|}$ has the entries:

$$[\tilde{\boldsymbol{\sigma}}(\boldsymbol{\eta}, \mathbf{q})]_e = \tilde{\sigma}(\eta_{f(e)}, \eta_{h(e)}, q_e).$$

Then, we obtain the nodal pressures p_v by solving the linear system (3.2b) as the right side of this linear system is fully determined by the topology of the network, the flow q_e and composition η_e on the edges and the given nodal pressure at node v^* . Moreover, the square matrix $A_{-v^*}^\top$ is regular, cf. [13], which completes the proof. \square

3.2 Steady States on Networks with One Cycle

In this section we discuss the existence of solutions to the mixture model (2.14) for networks with cycles. In particular, we prove the main result Theorem 3.6, the existence of solutions for networks with a single cycle. Moreover, we also comment on whether the result extends to networks with active elements such as compressors.

Theorem 3.6 (Existence of Solutions for Networks with One Cycle). *Let $\mathcal{G} = (\mathcal{V}, \mathcal{E})$ be a directed graph with exactly one cycle. Then the mixture model (2.14) admits at least one solution.*

The key idea to prove Theorem 3.6 is to cut an edge of the cycle, which results in a tree-shaped network for which we know that a unique solution exists (Theorem 3.5). The cut creates two new nodes that require boundary data, for which we introduce two parameters. As our aim is to show that the mixture model (2.14) admits a solution, we derive additional constraints that a solution for the cut networks must satisfy in order to be also a solution to the original one, and prove that there exist parameters that satisfy these constraints.

Before we prove Theorem 3.6, we derive an equivalent characterization of the solvability of the mixture model (2.14). At the end of this section, we utilize this characterization to conclude that the mixture model (2.14) admits at least one solution. We start by introducing the notion of a *cut graph* to formalize the process of cutting edges of a graph.

Definition 3.7 (Cut Graph, cf. [19, 32]). Let \mathcal{G} be a directed, connected graph and let $e^c = (f(e^c), h(e^c))$ be an edge of \mathcal{G} . Then the so-called *cut graph* $\mathcal{G}^c = (\mathcal{V}^c, \mathcal{E}^c)$ of \mathcal{G} with respect to e^c is defined by

$$\mathcal{V}^c = \mathcal{V} \cup \{v_{\text{cl}}, v_{\text{cr}}\}, \quad \mathcal{E}^c = (\mathcal{E} \setminus \{e^c\}) \cup \{e_{\text{cl}}, e_{\text{cr}}\},$$

where the nodes $v_{\text{cl}}, v_{\text{cr}} \notin \mathcal{V}$ are generated by cutting the edge e^c which splits into the two new edges $e_{\text{cl}} = (f(e^c), v_{\text{cl}})$ and $e_{\text{cr}} = (v_{\text{cr}}, h(e^c))$, see Figure 6 for a visualization.

Since our goal is to find solutions to the mixture model on the cut graph \mathcal{G}^c that are also solutions to the original graph \mathcal{G} , we assume that the boundary data for all old nodes $v \in \mathcal{V}$ remains the same. At the new nodes $v \in \{v_{\text{cl}}, v_{\text{cr}}\}$, solutions for the cut graph \mathcal{G}^c – indicated by the superscript c – must satisfy three conditions, in order to be solutions for the original graph \mathcal{G} as well:

$$\text{(c.i)} \quad b_{v_{\text{cl}}}^c = -b_{v_{\text{cr}}}^c, \quad \text{(c.ii)} \quad \eta_{v_{\text{cl}}}^c = \eta_{v_{\text{cr}}}^c, \quad \text{(c.iii)} \quad p_{v_{\text{cl}}}^c = p_{v_{\text{cr}}}^c.$$

The first condition (c.i) guarantees that the amount of gas leaving node v_{cl} is equal to the amount of entering node v_{cr} . One can also think of this condition as an invisible pipe connecting the nodes v_{cl} and v_{cr} , ensuring that the gas flow through the cut is constant. The condition (c.ii) and the condition (c.iii) ensure that the composition and the pressure are constant through the cut, respectively.

Next, we introduce appropriate boundary data for the newly introduced nodes v_{cl} and v_{cr} to guarantee the problem on the cut graph is well-defined and to ensure that the condition (c.i) is always satisfied. Therefore, we introduce the parameter $\lambda \in \mathbb{R}$ and set:

$$b_{v_{\text{cl}}}^c = \lambda \quad \text{and} \quad b_{v_{\text{cr}}}^c = -\lambda.$$

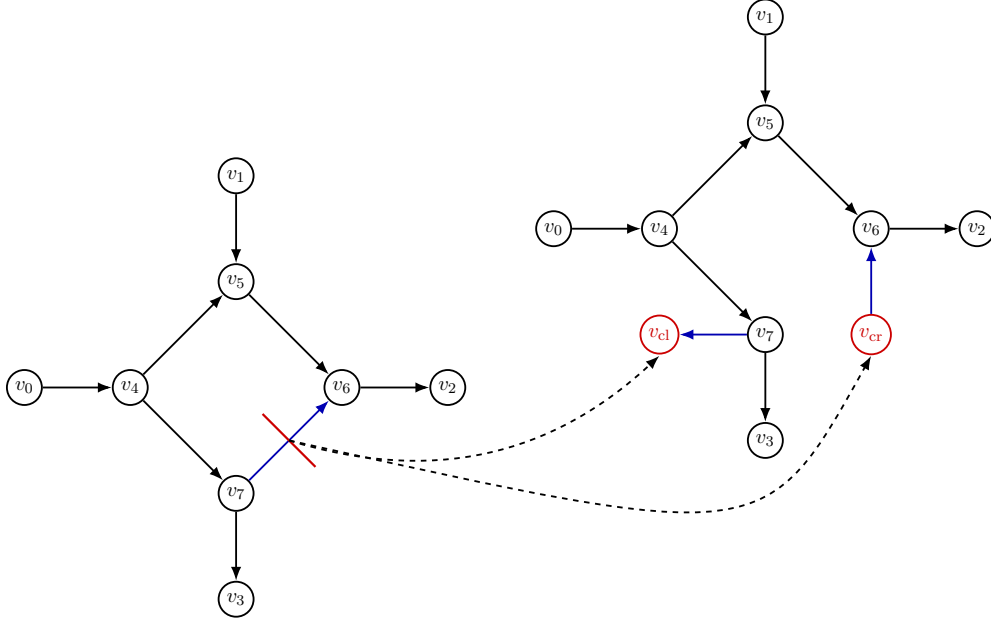


Figure 6: A graph with a single circle (left) and the resulting cut graph when cutting the blue edge (right).

Further, we introduce a second parameter $\mu \in [0, 1]$ to model the composition of the supply at the nodes v_{cl} and v_{cr} depending on the sign of λ . Then, the full set of boundary data for the gas flow model on the cut graph then reads:

$$p_{v^*}^c = p^*, \quad b_v^c = \begin{cases} b_v, & v \in \mathcal{V}, \\ -\lambda, & v = v_{cr}, \\ \lambda, & v = v_{cl}, \end{cases} \quad \text{and} \quad \zeta_v^c = \begin{cases} \zeta_v, & v \in \mathcal{V}_{<0}, \\ \mu, & v = v_{cr} \text{ and } \lambda \leq 0, \\ \mu, & v = v_{cl} \text{ and } \lambda > 0. \end{cases}$$

We also have to set the length, diameter, and friction factor of the edges $e \in \{e_{cl}, e_{cr}\}$ generated by the cut. We set the edge length to half the length of the cut edge e^c , i.e., we have $L^e = \frac{1}{2}L^{e^c}$ for $e \in \{e_{cl}, e_{cr}\}$. Since we assume that all edges have the same diameter and the same friction factor, this property transfers to the two new edges.

We rewrite the condition of constant composition and constant pressure through the cut by using the functions:

$$H_p: \mathbb{R} \times [0, 1] \rightarrow \mathbb{R}, \quad H_p(\lambda, \mu) = p_{v_{cr}}(\lambda, \mu)^2 - p_{v_{cl}}^c(\lambda, \mu)^2 \quad (3.3a)$$

$$H_\eta: \mathbb{R} \times [0, 1] \rightarrow \mathbb{R}, \quad H_\eta(\lambda, \mu) = \eta_{v_{cr}}^c(\lambda, \mu) - \eta_{v_{cl}}^c(\lambda, \mu), \quad (3.3b)$$

which measure the difference between the pressure and the composition at the new nodes, respectively. Notice that if the pipes are sufficiently short, cf. Equation (2.5), the condition $H_p(\lambda, \mu) = 0$ is equivalent to $p_{v_{cr}}(\lambda, \mu) = p_{v_{cl}}(\lambda, \mu)$. Then, the task of finding parameters λ and μ , which satisfy the constraints (c.i), (c.ii), and (c.iii), becomes:

$$\text{Find } (\lambda, \mu) \in \mathbb{R} \times [0, 1] \text{ such that } H_p(\lambda, \mu) = 0 \text{ and } H_\eta(\lambda, \mu) = 0,$$

which means we have to find a common root of H_p and H_η . With this derivation at hand, we obtain an equivalent characterization of the solvability of the steady-state gas flow model (2.14), which we capture in the following lemma.

Lemma 3.8. *Let $\mathcal{G} = (\mathcal{V}, \mathcal{E})$ be a directed graph. Then the following holds:*

$$\begin{array}{l} \text{The gas flow model (2.14)} \\ \text{has a solution.} \end{array} \Leftrightarrow \begin{array}{l} \text{The functions } H_p \text{ and } H_\eta \\ \text{have a common root.} \end{array}$$

Proof. Assume the steady-state gas flow model (2.14) has a solution q_e, η_v, p_v and let e^c be the cut edge. Then, by definition of H_p and H_η , these two functions have the common root:

$$\lambda^* = q_{e^c} \quad \text{and} \quad \mu^* = \begin{cases} \eta_{f(e^c)}, & \text{if } q_{e^c} \geq 0, \\ \eta_{h(e^c)}, & \text{if } q_{e^c} < 0. \end{cases}$$

Now suppose that H_p and H_η have a common root (λ^*, μ^*) . Then, we recover a solution to the gas flow model (2.14) by setting:

$$q_e = \begin{cases} q_e^c(\lambda^*, \mu^*), & e \in \mathcal{E} \setminus \{e^c\}, \\ \lambda^*, & e = e^c, \end{cases} \quad \eta_v = \eta_v^c(\lambda^*, \mu^*), \quad p_v = p_v^c(\lambda^*, \mu^*). \quad \square$$

In case the functions H_p and H_η have a common root, the solvability of the mixture model (2.14), i.e., Theorem 3.6, follows immediately with Lemma 3.8. Therefore, our next goal is to show that the functions H_p and H_η have a common root.

Lemma 3.9. *Let $\mathcal{G} = (\mathcal{V}, \mathcal{E})$ be a directed graph with one cycle and let $e^c \in \mathcal{E}$ be an edge belonging to the cycle. Further, let \mathcal{G}^c be the cut graph obtained by cutting the edge e^c . Then, there exists a tuple $(\lambda^*, \mu^*) \in \mathbb{R} \times [0, 1]$ such that*

$$H_p(\lambda^*, \mu^*) = 0 \quad \text{and} \quad H_\eta(\lambda^*, \mu^*) = 0,$$

where the functions H_p and H_η are defined in Equation (3.3), i.e., these two functions have at least one common root.

The idea of the proof of Lemma 3.9 is as follows:

- (i) For a fixed λ , we show that the function H_η admits a unique root $\mu_\eta(\lambda)$, which means $H_\eta(\lambda, \mu_\eta(\lambda)) = 0$ holds.
- (ii) Then, we restrict the function H_p to the root curve $\mu_\eta(\lambda)$ resulting in the scalar function $g(\lambda) = H_p(\lambda, \mu_\eta(\lambda))$. Then, we apply the intermediate value theorem to the function g to show that it admits at least one root, i.e., we have to show that
 - (a) the function g is continuous, and that
 - (b) there exist values λ^- and λ^+ such that $g(\lambda^-) \leq 0$ and $g(\lambda^+) \geq 0$.

In Figure 7, we provide an overview of the intermediate results required and group them into two categories corresponding to the two steps of the proof. In the following, we postpone the detailed proof to show the intermediate results first.

To show the two intermediate steps of the proof, we analyze the properties of the nodal composition η_v^c and the flow q_e^c on the edges, because both functions, H_p and H_η , can be

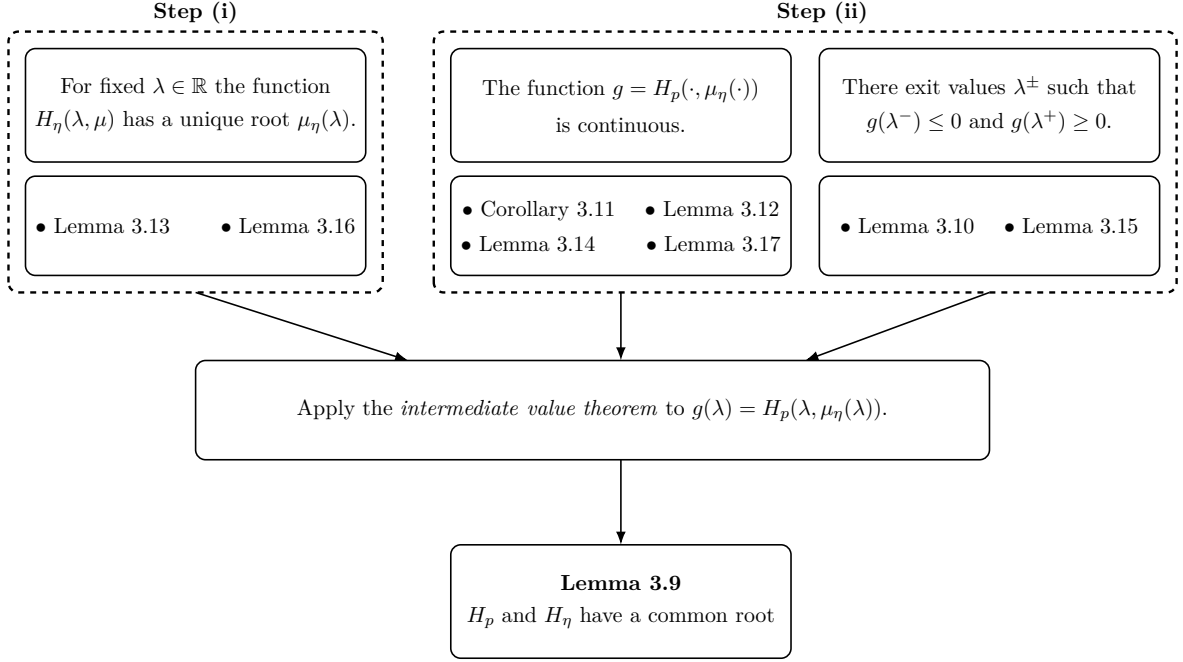


Figure 7: Overview and dependence of intermediate results to show Lemma 3.9.

written in terms of η_v^c and q_e^c . For the function H_η , this holds by definition. The function H_p describes the pressure loss between the node v_{cl} and the node v_{cr} . Hence, we invoke Lemma 2.4 to express H_p in terms of η_v^c and q_e^c , which results in:

$$H_p(\lambda, \mu) = \sum_{e \in \mathcal{E}_p} \tilde{\sigma}(\eta_{f(e)}^c(\lambda, \mu), \eta_{h(e)}^c(\lambda, \mu), q_e^c(\lambda)) a^c(v_e, e) q_e^c(\lambda) |a^c(v_e, e) q_e^c(\lambda)|, \quad (3.4)$$

where $\mathcal{E}_p \subseteq \mathcal{E}^c$ is the set of edges that belong to the path connecting v_{cl} and v_{cr} and v_e denotes the node of the edge e that is closer to the start node of the path.

Thus, besides analyzing the properties of the flow q_e^c and the nodal composition η_v^c , we also show how these properties carry over to the functions H_p and H_η , and how they contribute to the proof of Lemma 3.9.

3.2.1 Properties of the Flow and the Nodal Composition

We start by showing that the flow q_e^c on the edges of the former cycle of the network depends linearly on λ as this property is essential to that the function H_η admits a unique root, and that the function $\lambda \mapsto H_p(\lambda, \mu_\eta(\lambda))$ satisfies the requirements on the intermediate value theorem.

Lemma 3.10. *Let $\mathcal{G} = (\mathcal{V}, \mathcal{E})$ be a graph with one cycle and let $e^c \in \mathcal{E}$ be the cut edge belonging to the cycle $(\mathcal{C}, \mathcal{E}_\mathcal{C})$. Assume λ and μ are fixed. Then the flow q_e^c on the cut graph \mathcal{G}^c depends linearly on λ and can be written as:*

$$a^c(v_e, e) q_e^c(\lambda) = \gamma_e - \lambda \quad \text{for all } e \in (\mathcal{E}_\mathcal{C} \setminus \{e^c\}) \cup \{e_{cl}, e_{cr}\},$$

where the constants γ_e depend only on the loads b_v and v_e is the node of the edge e that is closer to the node v_{cr} (cf. Lemma 2.4 for the definition of v_e).

Proof. Since the graph \mathcal{G} has only one cycle that is cut, the cut graph \mathcal{G}^c is tree-shaped. Therefore, there exists exactly one path connecting the nodes v_{cl} and v_{cr} . We denote the path as a connected sub-graph $(\mathcal{P}, \mathcal{E}_{\mathcal{P}})$ of \mathcal{G}^c , where

$$\mathcal{P} = \mathcal{C} \cup \{v_{cl}, v_{cr}\} \quad \text{and} \quad \mathcal{E}_{\mathcal{P}} = \mathcal{E}_{\mathcal{C}} \setminus \{e^c\} \cup \{e_{cl}, e_{cr}\}. \quad (3.5)$$

The proof follows part of the proof of [19, Theorem 1]. Without loss of generality we assume that the path starts at node v_{cr} and ends at node v_{cl} . Every edge $e \notin \mathcal{E}_{\mathcal{P}}$ is part of a sub-tree of \mathcal{G}^c with one node in \mathcal{P} . As the loads b_v^c for nodes $v \notin \mathcal{P}$ are fixed and independent of λ , the flow on the edge $e \notin \mathcal{E}_{\mathcal{P}}$ is uniquely determined and independent of λ . Hence, only the flow values along the path $(\mathcal{P}, \mathcal{E}_{\mathcal{P}})$ can change when λ changes and we can redefine the loads for the nodes on the path:

$$b_v^{\mathcal{P}} := b_v^c - \sum_{e \in \mathcal{E}(v) \setminus \mathcal{E}_{\mathcal{P}}} a^c(v, e) q_e^c \quad \text{for } v \in \mathcal{P}.$$

Then, the conservation of mass, cf. Equation (2.14b), becomes $A^{\mathcal{P}} \mathbf{q}^{\mathcal{P}} = \mathbf{b}^{\mathcal{P}}$ where $A^{\mathcal{P}}$ is the incidence matrix of the sub-graph of the path and has a lower triangular structure:

$$A^{\mathcal{P}} = \begin{pmatrix} a^c(v_1, e_1) & & & & & & \\ a^c(v_2, e_1) & a^c(v_2, e_2) & & & & & \\ & a^c(v_3, e_2) & \ddots & & & & \\ & & \ddots & a^c(v_{p-2}, e_{p-2}) & & & \\ & & & a^c(v_{p-1}, e_{p-2}) & a^c(v_{p-1}, e_{p-1}) & & \\ & & & & a^c(v_p, e_{p-1}) & & \end{pmatrix},$$

where $p = |\mathcal{P}| = |\mathcal{E}_{\mathcal{P}}| + 1$. The numbering of the nodes indicates the order in which they are traversed by the path, i.e., $v_1 = v_{cr}$ and $v_p = v_{cl}$. An edge e_i connects the nodes v_i and v_{i+1} . The vector $\mathbf{q}^{\mathcal{P}}$ has entries corresponding to the flow values of the edges $e \in \mathcal{E}_{\mathcal{P}}$ and the vector $\mathbf{b}^{\mathcal{P}}$ entries corresponding to the redefined loads $b_v^{\mathcal{P}}$. Then, we apply forward substitution to the linear system and obtain:

$$a^c(v_i, e_i) q_{e_i}^c = \sum_{k=1}^i b_{v_k}^{\mathcal{P}} \quad \text{for } i = 1, \dots, p-1.$$

As the path starts at node $v_1 = v_{cr}$, we have $a^c(v_1, e_1) q_{e_1}^c = b_{v_1}^{\mathcal{P}} = -\lambda$. Further, the redefined loads $b_v^{\mathcal{P}}$ are independent of λ for $v \notin \{v_1 = v_{cl}, v_p = v_{cr}\}$, which leads to

$$a^c(v_i, e_i) q_{e_i}^c = -\lambda + \underbrace{\sum_{k=2}^i \left[b_{v_k} - \sum_{e \in \mathcal{E}(v_k) \setminus \mathcal{E}_{\mathcal{P}}} a(v_k, e) q_e^c \right]}_{=: \gamma_{e_i} \text{ which is independent of } \lambda} \quad \text{for } i = 1, \dots, p-1$$

$$\Leftrightarrow a^c(v_e, e) q_e^c = \gamma_e - \lambda \quad \text{for } e \in \mathcal{E}_{\mathcal{P}} = (\mathcal{E}_{\mathcal{C}} \setminus \{e^c\}) \cup \{e_{cl}, e_{cr}\}. \quad \square$$

With this representation of q_e^c for edges of the former cycle and the knowledge that the

flow is independent of λ for edges not belonging to the former cycle, it follows directly that the flow is continuous in λ .

Corollary 3.11 (Continuity of the Flow). *Let the requirements of Lemma 3.10 be satisfied. Then the flow q_e^c on the cut graph \mathcal{G}^c is continuous in λ for all edges $e \in \mathcal{E}^c$.*

Proof. The claim follows directly from the proof of Lemma 3.10 as q_e^c is independent of λ if $e \notin \mathcal{E}_C \cup \{e_{cl}, e_{cr}\}$ and linear in λ if $e \in \mathcal{E}_C \cup \{e_{cl}, e_{cr}\}$. \square

The continuity of q_e^c with respect to λ allows us to show that the nodal compositions η_v^c are also continuous. However, the roles of the nodes v_{cl} and v_{cr} depend on the sign of λ . That is, for $\lambda > 0$, the node v_{cl} is a demand node and v_{cr} a supply node, while for $\lambda < 0$, the roles are reversed. One can compare the switching of the sign to a supply station that suddenly becomes a consumer, in which case we anticipate the change, and thus, the composition at these nodes to be discontinuous for $\lambda = 0$.

Lemma 3.12 (Continuity of the Composition with respect to λ). *Let \mathcal{G} be a connected graph with a single cycle, $e^c \in \mathcal{E}$ an edge belonging to the cycle, \mathcal{G}^c the resulting cut graph. Assume $\mu \in [0, 1]$ is arbitrary, yet fixed. Then:*

- (i) *The nodal compositions η_v^c are continuous for $\lambda \in \mathbb{R} \setminus \{0\}$.*
- (ii) *The nodal compositions η_v^c are also continuous in $\lambda = 0$ for nodes $v \in \mathcal{V} \setminus \{v_{cl}, v_{cr}\}$.*

Proof. We prove the claim by using the concept of a topological ordering to traverse through the nodes of \mathcal{G}^c as the graph $\mathcal{G}_{\text{flow}}^c$ with then same nodes as cut graph \mathcal{G}^c but edges according to the flow direction, is tree-shaped and thus, has a topological ordering of its nodes.

The flow along the path connecting the nodes v_{cl} and v_{cr} only changes when λ changes. because the cut graph \mathcal{G}^c is tree-shaped. Lemma 3.10 allows to determine flow direction of an edge belonging to this path depending on λ as well as for which value of λ the flow of an edge becomes zero. We sort these roots in ascending order:

$$\gamma_{\min} = \tilde{\gamma}_1 < \dots < \tilde{\gamma}_{|\mathcal{E}_P|} = \gamma_{\max} \quad \text{where} \quad \{\gamma_e \mid e \in \mathcal{E}_P\} = \{\tilde{\gamma}_i \mid i = 1, \dots, |\mathcal{E}_P|\}.$$

Then, for a fixed i , the flow directions are the same for all $\lambda \in (\tilde{\gamma}_i, \tilde{\gamma}_{i+1})$. Thus, the topological ordering differs for each sub-interval $(\tilde{\gamma}_i, \tilde{\gamma}_{i+1})$ as the flow directions depend on λ . Now, we show the continuity of η_v^c with respect to λ on $(\tilde{\gamma}_i, \tilde{\gamma}_{i+1})$ by an induction over the position k in the topological ordering for a fixed, yet arbitrary index $i \in \{1, \dots, |\mathcal{E}_P|\}$.

The first node v in the ordering has to be a supply node where the composition is given through boundary data, i.e., $\eta_v^c = \zeta_v^c$ is constant and hence continuous in λ .

In the induction step, we assume that all compositions up to position k are continuous on the sub-interval and that v is the node at position $k + 1$. Then the composition η_v^c is given by:

$$\eta_v^c = \frac{\sum_{e \in \mathcal{E}(v)} \eta_{w_e}^c (a^c(v, e)q_e^c)^+ + \zeta_v^c (b_v^c)^-}{\sum_{e \in \mathcal{E}(v)} (a^c(v, e)q_e^c)^+ + (b_v^c)^-} \quad \text{where} \quad w_e = \begin{cases} f(e), & \text{if } v = h(e), \\ h(e), & \text{if } v = f(e). \end{cases}$$

Because the topological ordering is based on the graph with edge in the flow direction, the inflow comes from nodes previous in the ordering. Thus, by the induction assumption we know that the compositions $\eta_{w_e}^c$ and the flows q_e^c are continuous on the sub-interval and since $a^c(v, e)q_e^c \neq 0$ by definition of the sub-interval, we also never divide by zero. Hence, the

compositions η_v^c are continuous for $\lambda \neq \tilde{\gamma}_i$. The continuity for the intervals $(-\infty, \tilde{\gamma}_0)$ and $(\tilde{\gamma}_{|\mathcal{E}_{\mathcal{P}}|}, \infty)$ follows analogously.

It remains to prove the continuity in $\lambda = \tilde{\gamma}_i$. Let $\tilde{e} \in \mathcal{E}$ be an edge with $q_{\tilde{e}}(\tilde{\gamma}_i) = 0$. Then, the continuity of η_v^c in $\lambda = \tilde{\gamma}_i$ for nodes v not incident to \tilde{e} follows directly. For nodes incident to \tilde{e} two cases occur:

- (i) $a^c(v, \tilde{e})q_{\tilde{e}}^c < 0$ for $\lambda < \tilde{\gamma}_i \Rightarrow a^c(v, \tilde{e})q_{\tilde{e}}^c > 0$ for $\lambda > \tilde{\gamma}_i$, and
- (ii) $a^c(v, \tilde{e})q_{\tilde{e}}^c > 0$ for $\lambda < \tilde{\gamma}_i \Rightarrow a^c(v, \tilde{e})q_{\tilde{e}}^c < 0$ for $\lambda > \tilde{\gamma}_i$.

We demonstrate how to handle the first case since the second one is analogous. Let v be a node incident to \tilde{e} , then the following holds:

$$\begin{aligned} \lim_{\lambda \rightarrow \tilde{\gamma}_i^-} \eta_v^c(\lambda, \mu) &= \lim_{\lambda \rightarrow \tilde{\gamma}_i^-} \frac{\sum_{e \in \mathcal{E}(v) \setminus \{\tilde{e}\}} \eta_{w_e}^c (a^c(v, e)q_e^c)^+ + \zeta_v^c (b_v^c)^-}{\sum_{e \in \mathcal{E}(v) \setminus \{\tilde{e}\}} (a^c(v, e)q_e^c)^+ + (b_v^c)^-} \\ &= \frac{\sum_{e \in \mathcal{E}(v) \setminus \{\tilde{e}\}} \eta_{w_e}^c (a^c(v, e)q_e^c)^+ + \zeta_v^c (b_v^c)^-}{\sum_{e \in \mathcal{E}(v) \setminus \{\tilde{e}\}} (a^c(v, e)q_e^c)^+ + (b_v^c)^-} \\ &= \lim_{\lambda \rightarrow \tilde{\gamma}_i^+} \frac{\sum_{e \in \mathcal{E}(v)} \eta_{w_e}^c (a^c(v, e)q_e^c)^+ + \zeta_v^c (b_v^c)^-}{\sum_{e \in \mathcal{E}(v)} (a^c(v, e)q_e^c)^+ + (b_v^c)^-} = \lim_{\lambda \rightarrow \tilde{\gamma}_i^+} \eta_v^c(\lambda, \mu), \end{aligned}$$

which proves the continuity of η_v^c for $v \in \mathcal{V} \setminus \{v_{\text{cl}}, v_{\text{cr}}\}$. Notice, that the nodes v_{cr} and v_{cl} lead to a special case since both nodes are boundary nodes and their load b_v^c can change depending on the value of λ . In particular, both nodes can switch between supply and demand node when λ switches its sign. Hence, the compositions η_v^c are discontinuous in $\lambda = 0$ in general for $v \in \{v_{\text{cl}}, v_{\text{cr}}\}$. \square

The continuity of the composition with respect to μ follows from the fact that each nodal composition η_v is either independent of μ or depends linearly on it.

Lemma 3.13 (Continuity of the Composition with respect to μ). *Let \mathcal{G} be a connected graph with a single cycle, $e^c \in \mathcal{E}$ an edge belonging to the cycle, \mathcal{G}^c the resulting cut graph. Moreover, let $u \in \mathcal{V}_{<0}^c$ be a supply node with supply composition ζ_u^c and let q_e^c be a flow on the network satisfying Equation (2.14b). Then for every node $v \in \mathcal{V}^c$, one of the two cases apply:*

- (i) *The nodal composition η_v^c depends linearly on ζ_u^c .*
- (ii) *The nodal composition η_v^c is independent of ζ_u^c .*

Further, the nodal compositions are well-defined, meaning $\eta_v^c \in [0, 1]$ for all $v \in \mathcal{V}^c$, if the boundary data satisfies $\zeta_v^c \in [0, 1]$ for every supply node $v \in \mathcal{V}_{<0}^c$.

Proof. There exists a topological ordering of the nodes of $\mathcal{G}_{\text{flow}}^c$ since we cut the only cycle of \mathcal{G} and we can prove the claim by induction over the position k in the ordering.

The node at position $k = 1$ must be a supply node where $b_v^c < 0$ holds. Therefore, η_v^c is given directly by boundary data, which implies that η_v is independent of ζ_u^c if $v \neq u$ and linear in ζ_u^c if $v = u$. By choice of the boundary data, we have $\eta_v^c \in [0, 1]$.

Now, assume that the claim holds for all nodes up to position k in the ordering. Let v be the node at position $k + 1$. Then, two cases can apply: (a) v is a supply node, or (b) v is not.

The case (a) is analogous to the case $k = 1$. In case (b), the composition can be computed by

$$\eta_v^c = \frac{\sum_{e \in \mathcal{E}(v)} \eta_{w_e}^c (a^c(v, e)q_e^c)^+ + \zeta_v^c (b_v^c)^-}{\sum_{e \in \mathcal{E}(v)} (a^c(v, e)q_e^c)^+ + (b_v^c)^-} \quad \text{where} \quad w_e = \begin{cases} f(e), & \text{if } v = h(e), \\ h(e), & \text{if } v = f(e). \end{cases}$$

As the gas flows from nodes early in the ordering to nodes later in the ordering, we know by the induction assumption that the compositions $\eta_{w_e}^c$ are linear or independent of ζ_w^c and $\eta_{w_e}^c \in [0, 1]$. \square

3.2.2 Properties of the Functions H_p and H_η

The next step is to extend the results that hold for the flow q_e^c and composition η_v^c to the functions H_p and H_η since both functions depend on these variables, cf. Equation (3.3) and Equation (3.4). First, we show that the function H_p is continuous in λ and μ as the flow and the composition are continuous too.

Lemma 3.14 (Properties of H_p). *The function $H_p: \mathbb{R} \times [0, 1] \rightarrow \mathbb{R}$ is*

- (i) *linear in μ , i.e., continuous and monotone in μ ,*
- (ii) *continuous in λ , and*
- (iii) *constant in μ if $\lambda = 0$.*

Proof. The function H_p describes the pressure loss along the path connecting the nodes v_{cl} and v_{cr} . Hence, we invoke Lemma 2.4 to obtain an alternative expression of H_p :

$$H_p(\lambda, \mu) = \sum_{e \in \mathcal{E}_p} \tilde{\sigma}(\eta_{f(e)}^c(\lambda, \mu), \eta_{h(e)}^c(\lambda, \mu), q_e^c(\lambda)) a^c(v_e, e) q_e^c(\lambda) |a^c(v_e, e) q_e^c(\lambda)|,$$

where v_e is the node of the edge e that is closer to node v_{cl} . Since the cut graph \mathcal{G}^c is tree-shaped, the flow q_e^c is fully determined by the loads b_v^c . Thus, the flow q_e^c along the edges is only dependent on the parameter λ and independent of the parameter μ .

- (i) The linearity of H_p with respect to μ follows directly from the linearity of the composition η_v with respect to μ , cf. Lemma 3.13.
- (ii) The argument to show the continuity with respect to λ is similarly. The continuity in $\lambda \neq 0$ follows from the continuity of the flow (Corollary 3.11) and the continuity of the composition (Lemma 3.12). In order to prove also the continuity in $\lambda = 0$, we rewrite the function H_p as

$$H_p(\lambda, \mu) = \underbrace{\sum_{\substack{e \in \mathcal{E}_p \\ e \neq e_{cl}, e_{cr}}} \tilde{\sigma}(\eta_{f(e)}^c(\lambda, \mu), \eta_{h(e)}^c(\lambda, \mu), q_e^c(\lambda)) a^c(v_e, e) q_e^c(\lambda) |a^c(v_e, e) q_e^c(\lambda)|}_{\text{continuous in } \lambda=0 \text{ by Corollary 3.11 and Lemma 3.12}} + \underbrace{\tilde{\sigma}(\eta_{v_{cr}}^c(\lambda), \eta_{h(e_{cr})}^c(\lambda, \mu), \lambda) \lambda |\lambda| + \tilde{\sigma}(\eta_{f(e_{cl})}^c(\lambda, \mu), \eta_{v_{cl}}^c(\lambda), \lambda) \lambda |\lambda|}_{\eta_{v_{cl}}^c \text{ and } \eta_{v_{cr}}^c \text{ are in general discontinuous in } \lambda=0}.$$

Although, the compositions $\eta_{v_{\text{cl}}}^c$ and $\eta_{v_{\text{cr}}}^c$ are discontinuous at $\lambda = 0$ by Lemma 3.12, the function H_p is continuous at $\lambda = 0$ because terms of the form $\tilde{\sigma}(\eta_{f(e)}^c, \eta_{h(e)}^c, \lambda)\lambda|\lambda|$ are continuous at $\lambda = 0$ even if the compositions $\eta_{f(e)}^c$ and $\eta_{h(e)}^c$ are not. This is because the function $\tilde{\sigma}$ is bounded from above which leads to

$$\left| \tilde{\sigma}(\eta_{f(e)}^c, \eta_{h(e)}^c, \lambda)\lambda|\lambda| \right| \leq \frac{\lambda_{\text{Fr}} L^e}{D} \max\{\sigma_{\text{H}_2}^2, \sigma_{\text{NG}}^2\} \lambda^2 \longrightarrow 0 \quad \text{for } \lambda \longrightarrow 0.$$

Hence, the discontinuity vanishes for $\lambda = 0$ and H_p is continuous at every λ .

- (iii) At last, we prove that H_p is constant in μ if $\lambda = 0$. As the flow is fully determined by the loads, the dependence on the parameter μ enters through the mixing equation. Specifically, through the term $\mu\lambda^2$ when computing the nodal composition η_v^c . Hence, if $\lambda = 0$ the nodal compositions are independent of μ and we get $H_p(0, \mu) \equiv \text{const.}$ \square

Next, we identify for which values of λ the flow is either directed from node v_{cl} to node v_{cr} or vice versa. As the function H_p describes the pressure loss along the path connecting v_{cl} and v_{cr} , this allows us to determine the sign of H_p for these values of λ .

Lemma 3.15 (Unidirectional Flow). *Assume the requirements of Lemma 3.10 are satisfied and define $\gamma_{\min} = \min_{e \in \mathcal{C} \setminus \{e^c\}} \gamma_e$ and $\gamma_{\max} = \max_{e \in \mathcal{C} \setminus \{e^c\}} \gamma_e$. Then:*

- (i) *The gas flows from v_{cr} to v_{cl} if and only if $\lambda \geq \gamma_{\max}$, which implies $H_p(\lambda, \mu) \geq 0$.*
- (ii) *The gas flows from v_{cl} to v_{cr} if and only if $\lambda \leq \gamma_{\min}$, which implies $H_p(\lambda, \mu) \leq 0$.*

Proof. Since the requirements of Lemma 3.10 are satisfied, the cut graph \mathcal{G}^c is tree-shaped and thus there exists only one path connecting the nodes v_{cl} and v_{cr} . Consider the sub-graph of \mathcal{G}^c that forms the path between v_{cr} and v_{cl} which we denote by

$$(\mathcal{P}, \mathcal{E}_{\mathcal{P}}) \quad \text{where } \mathcal{P} = \mathcal{C} \cup \{v_{\text{cl}}, v_{\text{cr}}\} \quad \text{and} \quad \mathcal{E}_{\mathcal{P}} = (\mathcal{E}_{\mathcal{C}} \setminus \{e^c\}) \cup \{e_{\text{cl}}, e_{\text{cr}}\}.$$

We assume without loss of generality that the path starts at v_{cr} and ends at v_{cl} . Then the flow being directed from v_{cr} to v_{cl} translates into $a^c(v_e, e)q_e^c \leq 0$ and being directed in the opposite direction translates into $a^c(v_e, e)q_e^c \geq 0$ for all $e \in \mathcal{E}_{\mathcal{P}}$. Consider the first case. Then, by Lemma 3.10 we get

$$a^c(v_e, e)q_e^c = \gamma_e - \lambda \leq \gamma_e - \gamma_{\max} \leq 0 \quad \text{for all } e \in \mathcal{E}_{\mathcal{P}} \quad \Leftrightarrow \quad \lambda \geq \lambda_{\max}$$

which means that the gas flows from node v_{cr} to node v_{cl} . The node v_e is the node of the edge e which is closer to node v_{cr} . Now, we apply Lemma 2.4 which yields:

$$H_p(\lambda, \mu) = p_{v_{\text{cr}}}^c(\lambda, \mu)^2 - p_{v_{\text{cl}}}^c(\lambda, \mu)^2 \geq 0.$$

The second case follows analogously. \square

From Lemma 3.13, we know that the composition η_v^c depends linearly on μ . As the function H_η is the difference between two nodal compositions, it is clear that it also depends linearly on μ . We exploit this linearity in the next lemma to prove that H_η has a unique root.

Lemma 3.16 (Root Curves of H_η). *The function $H_\eta: \mathbb{R} \times [0, 1]$ with*

$$H_\eta(\lambda, \mu) = \eta_{v_{\text{cr}}}^c(\lambda, \mu) - \eta_{v_{\text{cl}}}^c(\lambda, \mu),$$

is linear in μ . Furthermore, for a fixed λ , the function H_η admits a unique root $\mu_\eta(\lambda)$. For $\lambda \in [\gamma_{\min}, \gamma_{\max}]$ the root is given by:

$$\mu_\eta(\lambda) = \begin{cases} \eta_{v_{\text{cr}}}^c(\lambda), & \lambda < 0, \\ \eta_{v_{\text{cl}}}^c(\lambda), & \lambda \geq 0. \end{cases}$$

Proof. The linearity of H_η for a fixed λ follows immediately from Lemma 3.13. Due to the linearity it is also clear that $H_\eta(\lambda, \mu) = 0$ has a unique solution for a fixed λ . The goal now is to determine the explicit solution to this equation for $\lambda \in [\gamma_{\min}, \gamma_{\max}]$. We distinguish between four cases:

- (i) $\lambda = \gamma_{\min}$, (ii) $\lambda \in (\gamma_{\min}, 0)$, (iii) $\lambda \in [0, \gamma_{\max})$, (iv) $\lambda = \gamma_{\max}$.

First, we consider the case $\lambda \in [0, \gamma_{\max})$. In this case, we know that v_{cr} is a supply node with composition $\eta_{v_{\text{cr}}}^c = \mu$ and that v_{cl} is a demand node with composition $\eta_{v_{\text{cl}}}^c(\lambda, \mu)$ due to the sign of λ . Then, the composition $\eta_{v_{\text{cl}}}^c$ is independent of μ .

Assume otherwise, then the flow along the path connecting v_{cr} and v_{cl} must be directed from v_{cr} to v_{cl} , which contradicts the assumption $\lambda \leq \gamma_{\max}$ due to Lemma 3.15. Thus, we determine the root of H_η for a fixed λ by

$$H_\eta(\lambda, \mu) = 0 \quad \Leftrightarrow \quad \mu - \eta_{v_{\text{cl}}}^c(\lambda) = 0 \quad \Leftrightarrow \quad \mu_\eta(\lambda) = \eta_{v_{\text{cl}}}^c(\lambda).$$

The case $\lambda \in (\gamma_{\min}, 0)$ follows analogously.

Next, we consider the case $\lambda = \gamma_{\max}$. Then the flow of at least one of the edges of the path connecting v_{cr} and v_{cl} , is zero. Furthermore, $a(v_e, e)q_e^c \leq 0$ holds for all edges e of the path. In this scenario, no flow from node v_{cr} can reach node v_{cl} since at least one edge along the path has flow zero, even though – technically – the flow is directed from v_{cr} to v_{cl} . Thus, the composition $\eta_{v_{\text{cl}}}^c$ is again independent of μ and we can compute the root as for the case $\lambda \in [0, \gamma_{\max})$. Again, the case $\lambda = \gamma_{\min}$ follows analogously. \square

The structure of the root curve μ_η of H_η for $\lambda \in [\gamma_{\min}, \gamma_{\max}]$ allows us directly to show that it is continuous since the root curve is given by the nodal composition either of the node v_{cl} or the node v_{cr} depending on the sign of λ .

Lemma 3.17 (Continuity of the Root Curve μ_η). *The root curve $\mu_\eta: [\gamma_{\min}, \gamma_{\max}] \rightarrow [0, 1]$ defined in Lemma 3.16 is continuous in $\lambda \in [\gamma_{\min}, \gamma_{\max}] \setminus 0$.*

Proof. The claim follows directly from Lemma 3.12. \square

Finally, we are equipped to prove that the two functions H_p and H_η have a common root (Lemma 3.9). We recall the structure of the idea of the proof and indicate where the results from Section 3.2.1 and Section 3.2.2 come into play.

- (i) For a fixed λ , Lemma 3.16 shows that the function H_η has a unique root $\mu_\eta(\lambda)$.
- (ii) Then, we restrict the function H_p to the root curve $\mu_\eta(\lambda)$ and apply the intermediate value theorem to the restricted function $g(\lambda) = H_p(\lambda, \mu_\eta(\lambda))$, which requires that

- (a) the function g is continuous (Lemmas 3.14 and 3.17), and that
- (b) there exist values λ^- and λ^+ such that $g(\lambda^-) \leq 0$ and $g(\lambda^+) \geq 0$ (Lemma 3.15).

In the following, we provide the detailed proof of Lemma 3.9.

Proof of Lemma 3.9. We distinguish between two cases: The case where $\lambda = 0$ lies on the boundary of $[\gamma_{\min}, \gamma_{\max}]$ and the case where $\lambda = 0$ lies on the boundary of the interval.

First, we consider the case where $\lambda = 0$ lies in the interior of $[\gamma_{\min}, \gamma_{\max}]$. From Lemma 3.16, it follows that the equation $H_\eta(\lambda, \mu_\eta(\lambda)) = 0$ has a unique solution $\mu_\eta(\lambda)$ for a fixed $\lambda \in [\gamma_{\min}, \gamma_{\max}]$. The idea of the proof is now to use the root curve μ_η to define an auxiliary function:

$$g: [\gamma_{\min}, \gamma_{\max}] \rightarrow \mathbb{R}, \quad g(\lambda) = H_p(\lambda, \mu_\eta(\lambda)),$$

and show that g has at least one root in $[\gamma_{\min}, \gamma_{\max}]$ by applying the intermediate value theorem. Because once we have a root λ^* of g , we set $\mu^* = \mu_\eta(\lambda^*)$. All that remains, is to verify the requirements of the intermediate value theorem:

- (a) g is continuous on $[\gamma_{\min}, \gamma_{\max}]$,
- (b) $g(\gamma_{\min}) \leq 0$ and $g(\gamma_{\max}) \geq 0$.

We start by proving the continuity of g . From Lemma 3.17, it follows that the root curve μ_η is continuous on $[\gamma_{\min}, \gamma_{\max}] \setminus \{0\}$. Furthermore, we know that H_p is continuous (Lemma 3.14), which immediately provides the continuity of g for $\lambda \neq 0$. Thus, it remains to show the continuity of g in $\lambda = 0$. Recall, that from Lemma 3.14, it also follows that $H_p(0, \cdot)$ is constant, i.e., there exists an $\alpha \in \mathbb{R}$ such that $H_p(0, \mu) = \alpha$ for all $\mu \in [0, 1]$ which leads to:

$$\begin{aligned} \lim_{\lambda \rightarrow 0^-} g(\lambda) &= \lim_{\lambda \rightarrow 0^-} H_p(\lambda, \mu_\eta(\lambda)) = H_p(0, \lim_{\lambda \rightarrow 0^-} \mu_\eta(\lambda)) = \alpha \\ \alpha &= H_p(0, \lim_{\lambda \rightarrow 0^+} \mu_\eta(\lambda)) = \lim_{\lambda \rightarrow 0^+} H_p(\lambda, \mu_\eta(\lambda)) = \lim_{\lambda \rightarrow 0^+} g(\lambda). \end{aligned}$$

After we have established the continuity of g , requirement (b) follows immediately from Lemma 3.15, which completes the proof for this case.

Next, we consider the case where $\lambda = 0$ lies on the boundary of $[\gamma_{\min}, \gamma_{\max}]$. Then either $\gamma_{\min} = 0$ or $\gamma_{\max} = 0$. Let us assume that $\gamma_{\min} = 0$ as the other case follows analogously. Since H_p is continuous on $[\gamma_{\min}, \gamma_{\max}]$ and constant in $\lambda = 0$, there exists an $\varepsilon > 0$ independent of μ such that

$$\text{sign}(H_p(0, \mu)) = \text{sign}(H_p(\varepsilon, \mu)).$$

Hence, we can apply the same argumentation to the interval $[\varepsilon, \gamma_{\max}]$ as for the case where $\lambda = 0$ lies in the interior of the interval $[\gamma_{\min}, \gamma_{\max}]$. \square

After we have proved Lemma 3.9, we automatically obtain that the mixture model (2.14) has at least one solution, which proves our main result, Theorem 3.6.

Proof of Theorem 3.6. Due to Lemma 3.8, the solvability of the mixture model (2.14) is equivalent to the functions H_p and H_η having at least one common root, which follows from Lemma 3.9 and thus proves the claim. \square

Remark 3.18. So far, we have considered (passive) networks with at most one cycle, but the argumentation can also be applied to networks with active elements such as compressors, as long as they are not in parallel or form cycles. Furthermore, the compressor ratio must be independent of the composition and flow.

For tree-shaped networks, the flows q_e and the compositions η_v are uniquely determined by the conservation of mass and the mixing at the nodes, regardless of whether the network contains active elements or not. Thus, a solution for the pressure p_v exists and is also unique for networks with compressors. To prove the existence of a solution for single cycle networks, we use the function H_p . For networks with one cycle and compressors outside the cycle, the structure of H_p is the same as in Equation (3.4). Therefore, proving the existence of solutions is identical to proving Theorem 3.6. If compressors are inside the cycle, the compressor ratios enter the function H_p , i.e., some summands are multiplied by the compressor ratios. Which summands are affected depends on the position of the compressors in the cut cycle. As the compressor ratios are constant, again, the idea of the proof of Theorem 3.6 still applies.

4 Numerical Examples

So far, we restricted our theoretical investigation to networks with at most one cycle and skipped networks with multiple cycles such as the diamond network shown in Figure 10. The idea to prove the existence of a solution for these kind of networks is to use an induction over the number of cycles in the network. In Section 3.2, we have presented the first induction step going from networks without cycles to networks with one cycle. However, networks with multiple cycles pose new challenges when performing the induction since the cut graph of such networks is no longer tree-shaped.

One consequence is that the flow q_e^c on the edges of the cut graph is not fully determined by the loads b_v^c , i.e., it also depends on the supply composition ζ_v^c and the fixed pressure p^* . As the flow q_e^c now depends on both parameters, λ and μ , the composition η_v^c at a node v becomes non-linear in μ . The function H_η inherits the non-linearity and it becomes unclear whether the equation $H_\eta(\lambda, \mu) = 0$ admits a (unique) solution for every $\lambda \in \mathbb{R}$. Thus, the analysis of the non-linearity and its influence on the solvability of $H_\eta(\lambda, \mu) = 0$ remains subject to further research.

Therefore, we dedicate this section to a numerical study, which purpose is twofold. On the one hand, we visualize the idea of the proof of Theorem 3.6 by computing the functions $H_p(\lambda, \mu)$ and $H_\eta(\lambda, \mu)$ and calculating the root curve $\mu_\eta(\lambda)$ for a sample network with exactly one cycle. On the other hand, we apply the idea of the proof to a network with multiple cycles to showcase that the idea might also be applicable to networks with multiple cycles instead of networks with one cycle only. In particular, we compute the restriction $H_p(\lambda, \mu_\eta(\lambda))$ and prove, again numerically, that this function has a unique root, which implies with Lemma 3.8 that the mixture model (2.14) admits at least one solution.

4.1 A Network with One Cycle

In this section, we compute the functions H_p and H_η , and the root curve μ_η for a sample network with only one cycle. Furthermore, we link the theoretical results of Section 3.2 to our numerical example. As a sample network we use the (cut) network displayed in Figure 6. This network has exactly one cycle, two supply nodes, v_0 and v_1 , and two demand nodes, v_2

and v_3 . At the remaining nodes, the mass is conserved, that is, i.e., $b_v = 0$. In Table 1 we provide the specific values of the boundary data.

Table 1: Boundary data at the nodes

supply		demand	pressure
composition	load		
$\zeta_{v_0} = \frac{3}{4}$	$b_{v_0} = 4$	$b_{v_2} = -2$	$p_{v_0} = p^* = 60$
$\zeta_{v_1} = \frac{1}{4}$	$b_{v_1} = 4$	$b_{v_3} = -6$	

We can narrow down the range of λ , for which the function H_p can become zero, to the interval $[\gamma_{\min}, \gamma_{\max}] = [-6, 2]$ due to Lemma 3.15 and the boundary data given in Table 1. Thus, we evaluate the functions H_p and H_η on the domain $[-6, 2] \times [0, 1]$. As the evaluation of these functions at a fixed point (λ, μ) requires the solution of the mixture model (2.14), we discretize the intervals $[-6, 2]$ and $[0, 1]$ by uniform grids of size $N_\lambda = 50$ and $N_\mu = 51$, respectively, and solve the mixture model (2.14) only at these grid points. To obtain a solution to the non-linear system corresponding to the mixture model (2.14), we invoke the Levenberg-Marquardt method. The resulting functions H_p and H_η are displayed in Figure 8.

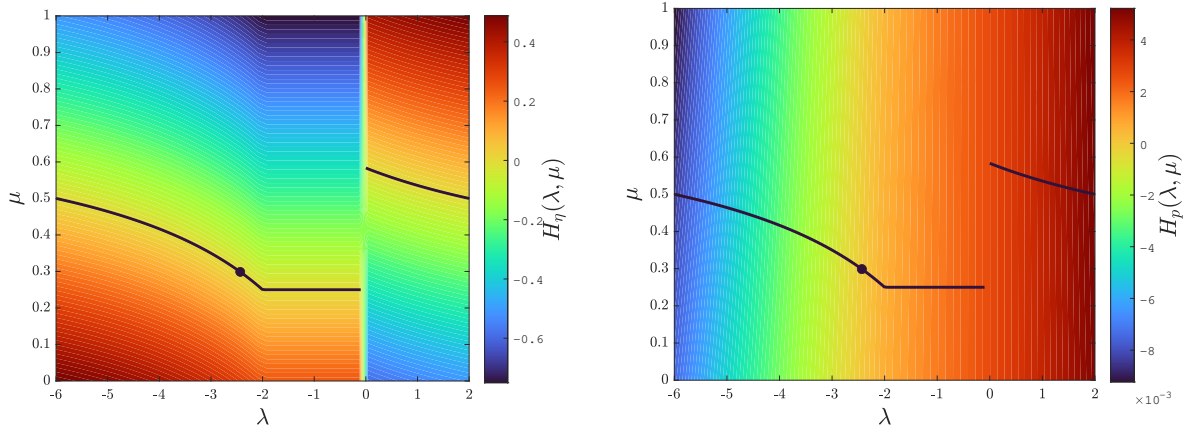


Figure 8: The functions $H_\eta(\lambda, \mu)$ (left) and $H_p(\lambda, \mu)$ (right) for the sample network in Figure 6. The black dot is the common root (λ^*, μ^*) , and the black line the root curve $\mu_\eta(\lambda)$.

First, we observe that the function H_η is discontinuous in $\lambda = 0$ for any value of $\mu \in [0, 1]$, cf. Lemma 3.12 and Lemma 3.16. This discontinuity is due to the sudden switch of roles at $\lambda = 0$ at the nodes v_{cl} and v_{cr} . For $\lambda > 0$, the node v_{cl} is a demand node and for $\lambda < 0$ it is a supply node. For the node v_{cr} it is vice versa. Moreover, we see that the function H_p is continuous in the entire domain, cf. Lemma 3.14 and that $H_p(\gamma_{\min}, \mu) \leq 0$ and $H_p(\gamma_{\max}, \mu) \geq 0$ for any value of $\mu \in [0, 1]$, cf. Lemma 3.15.

Besides the functions H_p and H_η , Figure 8 also shows the root curve μ_η . As the cut network in Figure 6 is tree-shaped, the flows q_e^c on the edges are fully determined by the loads b_v^c . Thus, the computation of the nodal compositions η_v^c is straightforward and by Lemma 3.16

we can compute the root curve μ_η explicitly:

$$\mu_\eta(\lambda) = \begin{cases} \frac{\zeta_{v_0} [b_{v_1} + b_{v_2} + \lambda] - \zeta_{v_1} b_{v_1}}{b_{v_2} + \lambda}, & \text{if } \lambda \in [b_{v_3}, b_{v_0} + b_{v_3}], \\ \zeta_{v_1}, & \text{if } \lambda \in [b_{v_0} + b_{v_3}, 0], \\ \frac{\zeta_{v_0} b_{v_0} - \zeta_{v_1} [b_{v_0} + b_{v_3} - \lambda]}{\lambda - b_{v_3}}, & \text{if } \lambda \in [0, -b_{v_2}]. \end{cases} \quad (4.1)$$

Notice that $b_{v_0} + b_{v_3} = -(b_{v_1} + b_{v_2})$ holds due to mass conservation and that $b_{v_0} + b_{v_3} \leq 0$ holds for the boundary data given in Table 1. Also note that the root curve μ_η is discontinuous in $\lambda = 0$ (unless $b_{v_0} = 0$), which is also visible in Figure 8 and backed-up by Lemma 3.17.

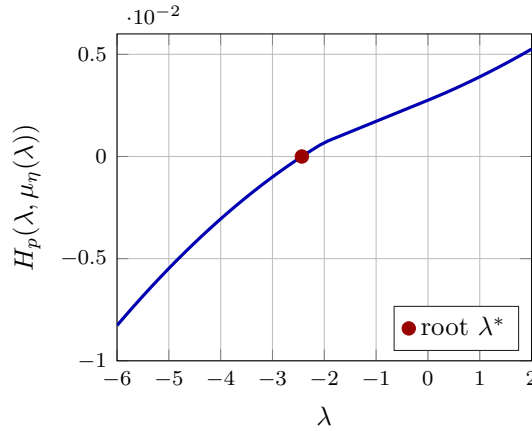


Figure 9: The function H_p restricted to the root curve $\mu_\eta(\lambda)$ for the sample network in Figure 6, resulting in the scalar function $g(\lambda) = H_p(\lambda, \mu_\eta(\lambda))$ from the proof of Theorem 3.6.

With this explicit representation, we can evaluate the function H_p along the root curve μ_η , i.e., the function $H_p(\lambda, \mu_\eta(\lambda))$, by solving the mixture model (2.14) on the cut graph. Again, to evaluate the function, we discretize the interval $[-6, 2]$ by a uniform grid of size $N_\lambda = 50$ and invoke the Levenberg-Marquardt method. The function $H_p(\lambda, \mu_\eta(\lambda))$ is displayed in Figure 9.

First of all, Figure 9 shows that the restriction $H_p(\lambda, \mu_\eta(\lambda))$ is continuous in $\lambda = 0$ even though the root curve μ_η is not, which follows from Lemma 3.9. Moreover, Figure 9 indicates that the function $H_p(\lambda, \mu_\eta(\lambda))$ is strictly monotonically increasing, which implies that its root λ^* is unique. Then, Lemma 3.8 would imply that solutions to the mixture model (2.14) are unique, which would be analogous to the „classic“ gas flow model involving only one gas instead of a mixture of multiple gases.

4.2 A Network with Multiple cycles

The subject of this section is to analyze whether the idea of the proof of Theorem 3.6 is also applicable to networks with multiple cycles. Therefore, we perform the same computations as in Section 4.1 but for the example of the diamond network shown in Figure 10. This network has the same supply and demand nodes as the network shown in Figure 6 but an additional

edge connecting the nodes v_5 and v_7 . We also assume the same boundary data as before.

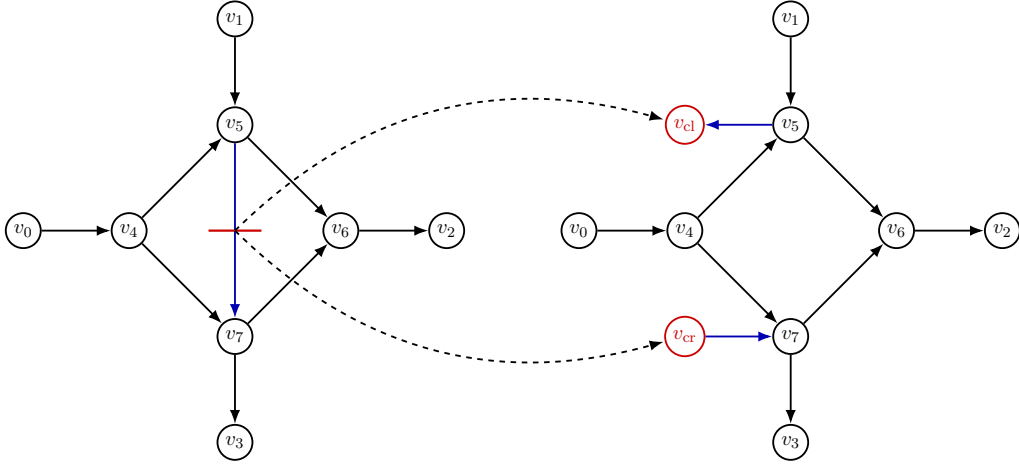


Figure 10: A graph with multiple, intertwined cycles (left) and the resulting cut graph when cutting the blue, inner edge (right).

Again, we can narrow down the range of λ , for which the function H_p becomes zero. However, this time we have to invoke [32, Lemma 14], which yields the interval:

$$\left[-\sum_{v \in \mathcal{V}} |b_v|, \sum_{v \in \mathcal{V}} |b_v| \right] = [-8, 8].$$

Before we delve into the analysis of the functions H_p and H_η , we emphasize the main difficulty when transferring the idea of the proof of Theorem 3.6 to networks with multiple cycles: The non-linear dependence of the composition η_v^c on μ , which makes the solving $H_\eta(\lambda, \mu) = 0$ with respect to μ more challenging. The non-linearity of the composition becomes evident in Figure 11, which shows the composition $\eta_{v_4}^c$ as a function of μ for different values of $\lambda \in [-8, 8]$. The color bar encodes the values of the parameter λ . Since the composition $\eta_{v_4}^c$ is constant for $\lambda \geq -0.5$, specifically $\eta_{v_4}^c(\lambda, \mu) \equiv 0.75$, we omit these values in the plot.

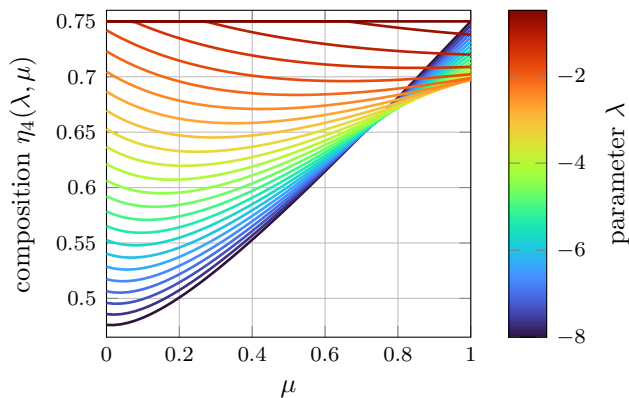


Figure 11: The nodal composition $\eta_{v_4}^c(\lambda, \mu)$ as a function of μ for different values of λ . The value of λ is encoded by the color bar.

Next, we analyze the functions H_p and H_η for the sample (cut) network shown in Figure 10. Both functions are displayed in Figure 12. Similar to the network with one cycle, we observe that the function H_η is discontinuous in $\lambda = 0$ for any value of $\mu \in [0, 1]$ and the function H_p has opposite signs for $\lambda = -8$ and $\lambda = 8$.

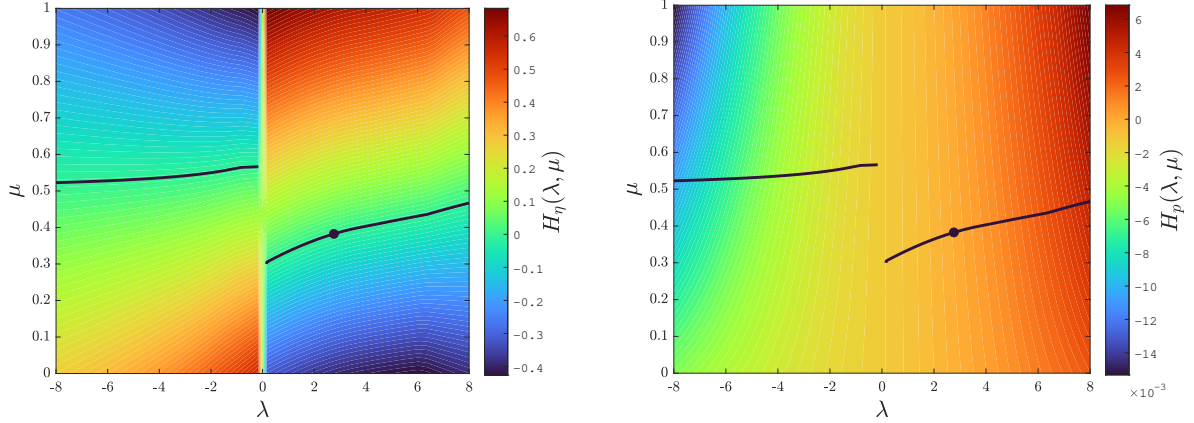


Figure 12: The functions $H_\eta(\lambda, \mu)$ (left) and $H_p(\lambda, \mu)$ (right) for the network in Figure 10. The black dot is the common root (λ^*, μ^*) , and the black line the root curve $\mu_\eta(\lambda)$.

In Figure 12, we also depict the root curve μ_η of the function H_η . The cut graph of the diamond network shown in Figure 6 is not tree-shaped. This makes the computation of the exact root curve more intricate and we compute an approximation of the exact root curve μ_η instead by extracting the coordinates of the level line $H_\eta(\lambda, \mu) = 0$ from the plot using Python's `get_paths()` function for contour plots. As for the network with one cycle, we see that the root curve μ_η is discontinuous in $\lambda = 0$, indicating that Lemma 3.12 also hold for networks with multiple cycles. Moreover, Figure 12 reveals that $H_\eta(\lambda, \mu) = 0$ has a unique solution for $\lambda \in [-8, 8]$ fixed.

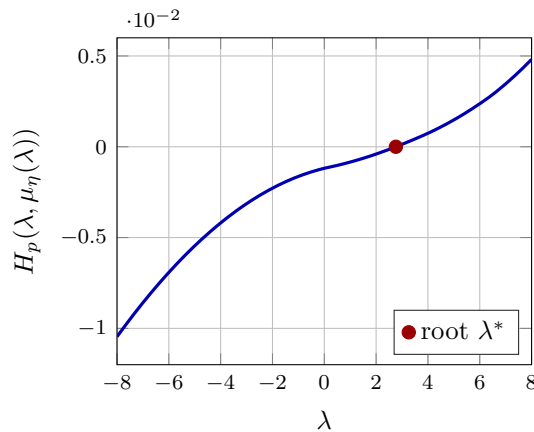


Figure 13: The functions $H_p(\lambda, \mu)$ (left) and $H_\eta(\lambda, \mu)$ (right) for the network in Figure 10. The black dot is the common root (λ^*, μ^*) , and the black line the root curve $\mu_\eta(\lambda)$.

The approximation of the root curve μ_η allows us to compute the function $H_p(\lambda, \mu_\eta(\lambda))$ by evaluating the function H_p at the corresponding coordinates. We provide the result in Figure 13. Again the function $H_p(\lambda, \mu_\eta(\lambda))$ is continuous in $\lambda = 0$ despite the discontinuity

of the root curve μ_η . Furthermore, we observe that $H_p(\lambda, \mu_\eta(\lambda))$ is strictly monotonically increasing with a unique root λ^* , implying that the solution of the mixture model (2.14) is unique, cf. Lemma 3.8.

In summary, the numerical experiments suggest that the idea of the proof of Theorem 3.6 also applies to networks with multiple cycles. However, to successfully extend the proof, we need to rigorously prove that $H_\eta(\lambda, \mu) = 0$ admits a unique solution for these types of networks.

5 Conclusion, Discussion and Future Work

In this paper we have analyzed the steady state problem of hydrogen blended natural gas transport in pipeline networks. We have clarified the differences to pure natural gas transport and discussed the existence and uniqueness of solutions on networks. For tree-shaped networks, we can compute unique flows by the mass conservation a priori, which guarantees the existence of a (unique) solution. For networks including a cycle, we have applied a cutting edge approach in order to show the existence of a solution. Cutting an edge in the cycle results in a tree-shaped graph with two new nodes and edges, and two additional coupling equations. We have shown that admissible solutions on the cut network exists which also meets the two additional coupling equations. This implies the existence of a solution for the graph with a cycle.

The uniqueness of a solution for tree-structured networks follows by the fact, that the flow direction is a priori given and thus, it is also a priori clear which node determines the composition on an edge. For networks including cycles, the composition of the gas on the edges in the cycle depends on the flow direction, leading to discontinuities in the mixing condition as discussed in Section 3.2. A natural extension of this work includes analyzing the discontinuities and thus also the uniqueness of a solution on networks with a cycle.

Additionally, considering optimization problems that involve hydrogen blends offer a valuable direction for future research. Such problems could explore optimal blending ratios, operational settings, or cost efficiencies while ensuring safety and regulatory standards. Even though the simulation and numerical optimization results presented in [1, 7, 20, 21, 28, 29] are promising, the research on the theoretical analysis of optimization problems that involve hydrogen blended natural gas transport is still very limited.

6 Acknowledgment

Simone Göttlich was supported by the German Research Foundation (DFG) under grant GO 1920/11-1 and 12-1.

References

- [1] L. S. Baker, S. R. Kazi, R. B. Platte, and A. Zlotnik. “Optimal Control of Transient Flows in Pipeline Networks with Heterogeneous Mixtures of Hydrogen and Natural Gas”. In: *2023 American Control Conference (ACC)* (2023), pp. 1221–1228. DOI: 10.23919/ACC55779.2023.10156571.

- [2] M. Banda, M. Herty, and A. Klar. “Coupling Conditions for Gas Networks governed by the Isothermal Euler Equations”. In: *Netw. Heretog. Media* 1.2 (2006), pp. 295–314.
- [3] M. Banda, M. Herty, and A. Klar. “Gas Flow in Pipeline Networks”. In: *Netw. Heretog. Media* 1.1 (2006), pp. 41–56.
- [4] J. Bang-Jensen and G. Z. Gutin. *Digraphs: Theory, Algorithms and Applications*. Springer London, 2008. DOI: 10.1007/978-1-84800-998-1.
- [5] R. B. Bapat. *Graphs and Matrices*. Springer, 2010. DOI: 10.1007/978-1-84882-981-7.
- [6] A. Bermúdez and M. Shabani. “Numerical simulation of gas composition tracking in a gas transportation network”. In: *Energy* 247 (2022). DOI: 10.1016/j.energy.2022.123459.
- [7] P. Börner, M. E. Pfetsch, and S. Ulbrich. “Modeling and optimization of gas mixtures on networks”. In: 2024. URL: %5Curl%7Bhttps://opus4.kobv.de/opus4-trr154/frontdoor/index/index.html%7D.
- [8] D. Bothe and W. Dreyer. “Continuum thermodynamics of chemically reacting fluid mixtures”. In: *Acta Mech.* 226 (2015), pp. 1757–1805.
- [9] Bundesregierung. *Energy from climate-friendly gas*. 2024. URL: %5Curl%7Bhttps://www.bundesregierung.de/breg-de/themen/energie/energie-und-klima/energie-und-klima-2024%7D.
- [10] P. Domschke, B. Hiller, J. Lang, and C. Tischendorf. *Modellierung von Gasnetzwerken: Eine Übersicht*. Tech. rep. 2717. Technische Universität Darmstadt, 2017. URL: %5Curl%7Bhttp://www3.mathematik.tu-darmstadt.de/fb/mathe/preprints.html%7D.
- [11] European Commission. *A hydrogen strategy for a climate-neutral Europe*. 2020. URL: %5Curl%7Bhttps://energy.ec.europa.eu/system/files/2020-07/hydrogen_strategy_0.pdf%7D.
- [12] European Hydrogen Backbone. *Five hydrogen supply corridors for Europe in 2030 - Executive Summary*. 2022. URL: %5Curl%7Bhttps://ehb.eu/files/downloads/EHB-Supply-corridors-2022.pdf%7D.
- [13] C. Gotzes, H. Heitsch, R. Henrion, and R. Schultz. “On the quantification of nomination feasibility in stationary gas networks with random load”. In: *Mathematical Methods of Operations Research* 84 (2016), pp. 427–457.
- [14] G. Guandalini, P. Colbertaldo, and S. Campanari. “Dynamic modeling of natural gas quality within transport pipelines in presence of hydrogen injections”. In: *Applied Energy* 185 (2 2017), pp. 1712–1723.
- [15] M. Gugat and J. Giesselmann. “An Observer for Pipeline Flow with Hydrogen Blending in Gas Networks: Exponential Synchronization”. In: *SIAM J. Control Optim.* 62.4 (2024), pp. 2273–2296.
- [16] M. Gugat, F. M. Hante, M. Hirsch-Dick, and G. Leugering. “Stationary States in Gas Networks”. In: *Networks and Heterogeneous Media* 10.2 (2015), pp. 295–320.
- [17] M. Gugat and M. Schuster. “Stationary Gas Networks with Compressor Control and Random Loads: Optimization with Probabilistic Constraints”. In: *Math. Prob. Eng. (Article ID 7984079)* (2018).
- [18] M. Gugat and S. Ulbrich. “Lipschitz Solutions of Initial Boundary Value Problems for Balance Laws”. In: *Math. Models Methods Appl. Sci.* 28.5 (2018), pp. 921–951.
- [19] M. Gugat, R. Schultz, and D. Wintergerst. “Networks of pipelines for gas with nonconstant compressibility factor: stationary states”. In: *Computational and Applied Mathematics* 37 (2018), pp. 1066–1097. DOI: 10.1007/s40314-016-0383-z.

- [20] S. R. Kazi, K. Sundar, S. Srinivasan, and A. Zlotnik. “Modeling and optimization of steady flow of natural gas and hydrogen mixtures in pipeline networks”. In: *International Journal of Hydrogen Energy* 54 (2024). DOI: 10.1016/j.ijhydene.2023.12.054.
- [21] S. R. Kazi, K. Sundar, and A. Zlotnik. “Dynamic Optimization and Optimal Control of Hydrogen Blending Operations in Natural Gas Networks”. In: *arXiv* (2024).
- [22] T. Koch, B. Hiller, M. E. Pfetsch, and L. Schewe. *Evaluating Gas Network Capacities*. MOS-SIAM, 2015.
- [23] K. Kumar, G. John, L. Lim, K. Seeger, M. Wakabayashi, and G. Kawamura. *Green Hydrogen in Asia: A Brief Survey of Existing Programmes and Projects*. 2023. URL: %5Curl%7Bhttps://www.orrick.com/en/Insights/2023/07/Green-Hydrogen-in-Asia-A-Brief-S
- [24] J. Málek and O. Souček. “A thermodynamic framework for heatconducting flows of mixtures of two interacting fluids”. In: *ZAMM Z. Angew. Math. Mech.* 102 (2022), Paper No. e202100389.
- [25] Office of Energy Efficiency & Renewable Energy. *Hydrogen: A Clean, Flexible Energy Carrier*. 2017. URL: %5Curl%7Bhttps://www.energy.gov/eere/articles/hydrogen-clean-flexible
- [26] M. Schmidt, M. Steinbach, and B. Willert. “High Detail Stationary Optimization Models for Gas Networks: Validation and Results”. In: *Optim. Eng.* 16.1 (2014).
- [27] M. Schuster, E. Strauch, M. Gugat, and J. Lang. “Probabilistic Constrained Optimization on Flow Networks”. In: *Optim. Eng.* 23 (2022), pp. 1–50.
- [28] M. Sodwatana, S. R. Kazi, K. Sundar, A. Brandt, and A. Zlotnik. “Locational Marginal Pricing of Energy in Pipeline Transport of Natural Gas and Hydrogen with Carbon Offset Incentives”. In: *arXiv* (2024).
- [29] M. Sodwatana, S. R. Kazi, K. Sundar, and A. Zlotnik. “Optimization of Hydrogen Blending in Natural Gas Networks for Carbon Emissions Reduction”. In: *2023 American Control Conference (ACC)* (2023), pp. 1229–1236. DOI: 10.23919/ACC55779.2023.10156202.
- [30] S. Srinivasan, K. Sundar, V. Gyrya, and A. Zlotnik. “Numerical Solution to the Steady-State Network Flow Equations for a Non-Ideal gas”. In: *IEEE Trans. Control Netw. Syst.* 10 (3 2022), pp. 1449–1461.
- [31] U.S. Department of Energy, OCED. *Multi-Year Program Plan*. 2023. URL: %5Curl%7Bhttps://www.ener
- [32] D. Wintergerst. “Optimization on Gas Networks under Stochastic Boundary Conditions”. PhD thesis. FAU Erlangen, 2019.
- [33] A. Witkowski, A. Rusin, M. Majkut, and K. Stolecka. “Analysis of compression and transport of the methane/hydrogen mixture in existing natural gas pipelines”. In: *International Journal of Pressure Vessels and Piping* 166 (2018), pp. 24–34.